EDGEWOOD CHEMICAL BIOLOGICAL CENTER
U.S. ARMY RESEARCH, DEVELOPMENT AND ENGINEERING COMMAND
Aberdeen Proving Ground, MD 21010-5424

ECBC-TR-1496

INVESTIGATION OF THE METABOLIC BIOTRANSFORMATION OF CCK-4 IN LIVER MICROSOMES OF HUMAN, MONKEY, RAT, AND MOUSE USING ULTRA-PERFORMANCE LIQUID CHROMATOGRAPHY–HIGH-RESOLUTION MASS SPECTROMETRY

Li Kong
Frederic Berg

RESEARCH AND TECHNOLOGY DIRECTORATE

July 2018

Disclaimer

The findings in this report are not to be construed as an official
Department of the Army position unless so designated by other authorizing documents.

REPORT DOCUMENTATION PAGE

Form Approved
OMB No. 0704-0188

1. REPORT DATE *(DD-MM-YYYY)*	**2. REPORT TYPE**	**3. DATES COVERED** *(From - To)*
XX-07-2018	Final	Dec 2016 – Jun 2017

4. TITLE AND SUBTITLE
Investigation of the Metabolic Biotransformation of CCK-4 in Liver Microsomes of Human, Monkey, Rat, and Mouse Using Ultra-Performance Liquid Chromatography–High-Resolution Mass Spectrometry

5a. CONTRACT NUMBER

5b. GRANT NUMBER

5c. PROGRAM ELEMENT NUMBER

6. AUTHOR(S)
Li, Kong and Berg, Frederic

5d. PROJECT NUMBER
CB 3662

5e. TASK NUMBER

5f. WORK UNIT NUMBER

7. PERFORMING ORGANIZATION NAME(S) AND ADDRESS(ES)
Director, ECBC, ATTN: RDCB-DRC-C, APG, MD 21010-5424

8. PERFORMING ORGANIZATION REPORT NUMBER
ECBC-TR-1496

9. SPONSORING / MONITORING AGENCY NAME(S) AND ADDRESS(ES)
Defense Threat Reduction Agency, Joint Science and Technology Office, 8725 John J. Kingman Road, MSC 6201, Fort Belvoir, VA 22060-6201

10. SPONSOR/MONITOR'S ACRONYM(S)
DTRA JSTO

11. SPONSOR/MONITOR'S REPORT NUMBER(S)

12. DISTRIBUTION / AVAILABILITY STATEMENT
Approved for public release: distribution unlimited.

13. SUPPLEMENTARY NOTES

14. ABSTRACT:
The goal of this study was to establish cholecystokinin tetrapeptide (CCK-4) metabolic stability in liver microsomes from four species (human, monkey, rat, and mouse) and identify and characterize CCK-4 metabolites using liquid chromatography–tandem mass spectrometry. Endogenous peptide metabolism is not well documented, and this is particularly true for neuropeptide CCK-4. In vitro, the metabolism of CCK-4 followed first-order kinetics, and the half-lives were 51.7, 36.7, 27.3, and 36.7 min for human (HLM), monkey (MyLM), rat (RLM), and mouse (MsLM) liver microsomes, respectively. The half-life of CCK-4 in HLMs was greater than that in MyLMs, RLMs, and MsLMs, which suggested that CCK-4 was metabolically more stable in HLMs. The degradation of CCK-4 was correlated with rapidly appearing metabolites in the incubation mixture, which suggested that the metabolites would be present in the systemic circulation. Six major metabolites were identified and quantified, and the measured metabolite concentrations indicated that significant differences in the CCK-4 metabolic profile exist between species.

15. SUBJECT TERMS
Cholecystokinin tetrapeptide (CCK-4) Liver microsomes Metabolism Biotransformation

16. SECURITY CLASSIFICATION OF:			**17. LIMITATION OF ABSTRACT**	**18. NUMBER OF PAGES**	**19a. NAME OF RESPONSIBLE PERSON**
a. REPORT	**b. ABSTRACT**	**c. THIS PAGE**			Renu B. Rastogi
U	U	U	UU	44	**19b. TELEPHONE NUMBER** *(include area code)* (410) 436-7545

Blank

PREFACE

The work described in this report was authorized under project number CB 3662 as administered by the Defense Threat Reduction Agency, Joint Science and Technology Office. The work was started in Dec 2016 and completed in June 2017.

The use of either trade or manufacturers' names in this report does not constitute an official endorsement of any commercial products. This report may not be cited for purposes of advertisement.

This report has been approved for public release.

Blank

CONTENTS

FIGURES

TABLES

Blank

INVESTIGATION OF THE METABOLIC BIOTRANSFORMATION OF CCK-4 IN LIVER MICROSOMES OF HUMAN, MONKEY, RAT, AND MOUSE USING ULTRA-PERFORMANCE LIQUID CHROMATOGRAPHY–HIGH-RESOLUTION MASS SPECTROMETRY

1. INTRODUCTION

Cholecystokinin (CCK) constitutes a family of homologous peptides that are 4–58 amino acids in length and derived from their precursor, preprocholecystokinin.[1] Cholecystokinin tetrapeptide CCK-4 (Trp–Met–Asp–Phe–NH_2) and its receptor are present in the mammalian brain and peripheral tissues. In the brain, CCK-4 acts primarily as an anxiogenic substance, although it retains some gastrointestinal effects.[2] CCK-4 reliably causes severe anxiety symptoms when administered to humans in a dose of as little as 50 μg,[3] and it is commonly used in scientific research to induce panic attacks for the purpose of testing new anxiolytic drugs.[4–8]

Little is known about the metabolism of CCK-4 after it is ingested. In the present work, the metabolic stability of CCK-4, as well as metabolite profiling and characterization, were investigated using ultra-performance liquid chromatography–high-resolution mass spectrometry (UPLC–HRMS). In this report, the in vitro metabolism and phase I biotransformation pathways of CCK-4 in human, monkey, rat, and mouse liver microsomes are described. In vitro metabolism studies are a valuable tool to predict in vivo metabolism. The aims of this study were (1) to investigate the in vitro metabolism of CCK-4 in human, monkey, rat, and mouse liver microsomes, and to establish the time and protein linearity; (2) to profile the metabolites; (3) to identify the metabolites; and (4) to elucidate the biotransformation pathway.

2. MATERIALS AND METHODS

2.1 Chemicals and Reagents

CCK-4 and radiolabeled CCK-4 (^{13}C, ^{15}N) were obtained from Las Alamos National Laboratory (Los Alamos, NM). Trifluoroacetic acid (TFA), monobasic potassium phosphate, potassium phosphate dibasic, NADPH (β-nicotinamide adenine dinucleotide 2'-phosphate reduced tetrasodium salt hydrate), magnesium chloride, tryptophan, and ammonium acetate were purchased from Sigma-Aldrich (St. Louis, MO). OmniSolv LC–MS acetonitrile and methanol (EMD Millipore; Burlington, MA) and B&J brand high-purity water were purchased from VWR International (Radnor, PA). The structure of CCK-4 is as follows:

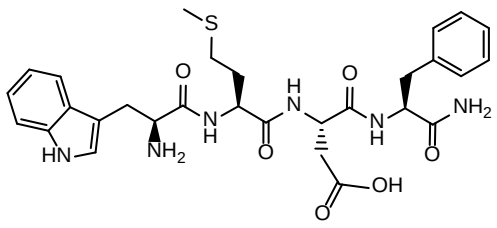

2.2 Microsomal Sources

Human (HLM), monkey (MyLM), rat (RLM), and mouse (MsLM) liver microsomes were purchased from XenoTech, LLC (Lenexa, KS). HLMs were derived from a mixed gender pool of 50 donors. MyLMs, RLMs, and MsLMs were prepared from mixed gender pools of rhesus monkeys (13 donors), Sprague Dawley rats (605 donors), and CD-1 mice (1520 donors), respectively. The total protein contents, cytochrome P-450 concentrations, and specific activities of different P-450 isoforms were supplied by the manufacturer. The protein concentrations for HLMs, MyLMs, RLMs, and MsLMs were each 20 mg/mL, and the total P-450 concentrations were 0.487, 1.288, 0.621, and 0.868 nmol/mg, respectively. All microsomes were stored at –80 °C until used.

2.3 Establishing Time and Protein Linearity for HLM, MyLM, RLM, and MsLM Incubations

Pooled HLMs, MyLMs, RLMs, and MsLMs were thawed and diluted with 100 mM potassium phosphate buffer (pH 7.4). Microsomal protein concentrations in the final reaction mixtures were 0.05, 0.1, 0.25, 0.5, 1.0, 1.5, and 2.0 mg/mL. CCK-4 at 5 µM was added into specified incubation vessels. Incubation mixtures were pre-warmed in the water bath at 37 °C for 3 min. The reactions were initiated by adding NADPH (2 mM) containing 3 mM $MgCl_2$ to each sample. The assays were performed in a shaking water bath at 37 °C and were conducted in triplicate. The total sample volume was 100 µL. The incubation times were 0, 5, 10, 20, 30, and 60 min. After the designated incubation time, an equal volume of ice-cold methanol containing an internal standard (radiolabeled CCK-4 at 1 µg/mL) was added to arrest the metabolic reaction. Samples were stored at –80 °C until analysis by liquid chromatography–tandem mass spectrometry (LC–MS/MS). Negative-control incubations were performed in triplicate under identical conditions for 0, 30, and 60 min. The negative-control microsomes had a 0.5 mg/mL protein concentration and had been boiled for 2 min. For the positive control, 7-ethoxycoumarin (5 µM) was incubated with liver microsomes at a 0.5 mg/mL protein concentration for 0, 15, and 30 min in triplicate. A vehicle control of blank liver microsomes without CCK-4 was incubated for 0 and 60 min in duplicate to determine the endogenous components in HLMs, MyLMs, RLMs, and MsLMs.

In contrast with the kinetic investigations, 25 µM of CCK-4 was used as the substrate concentration for qualitative analysis, to enhance the signal intensity of the formed metabolites, and was incubated for 0, 20, 40, and 60 min in triplicate. Degradation metabolites were identified by comparing chromatograms from vehicle-control and negative-control incubations to those from incubations in the presence of NADPH.

2.4 Sample Preparation

The incubation samples removed from the –80 °C freezer were thawed, vortexed, and centrifuged in an Eppendorf centrifuge (2250 ×*g* at 4 °C for 10 min). The supernatant was transferred to a UPLC vial and analyzed by UPLC–HRMS.

2.5 Metabolite Separation and Identification

Chromatographic separation of the metabolites was achieved by using a Thermo Fisher Scientific (San Jose, CA) UPLC-HRMS system that consisted of a Dionex UltiMate 3000 XRS open autosampler, Dionex UltiMate 3000 RSLCnano pumps, and an Orbitrap Fusion Tribrid mass spectrometer. Data were acquired and analyzed with Xcalibur software (Thermo Fisher Scientific). The peak area ratios of test compounds to internal standard were used for calculation in all experiments. The mean value of triplicate determinations was plotted versus the incubation times with different protein loadings. The initial concentration of CCK-4 in each incubation was designated as 100%, and all subsequent concentrations were expressed as a percentage of the initial concentration. CCK-4 was considered to be stable as long as the drug concentrations remained greater than 85% of their initial concentration at the end of the 60 min incubation period used in this study. Two UPLC methods were used for the quantitation and separation. The mobile phase consisted of 10 mM ammonium acetate with 0.05% TFA (A) and acetonitrile with 0.05% TFA (B). Quantitation was performed using a 50 × 2.1 mm Kinetex 1.7 µm EVO C18 column (Phenomenex, Inc.; Torrance, CA) and the following linear gradient conditions: 0 min, 5% B; 1.0 min, 5% B; 2.5 min, 95% B; 4.9 min, 95% B; 5.0 min, 5% B, and then equilibrated until 6 min. Metabolite separation was achieved using 100 × 2.1 mm Kinetex 1.7 µm EVO C18 column and the following linear gradient conditions: 0 min, 2% B; 4 min, 2% B; 20 min, 30% B; 36 min, 95% B; 38 min, 95% B; 38.1 min, 2% B, and then equilibrated until 40 min. A 10 µL sample was injected for both quantitation and metabolite identification. The UPLC flow rate was 280 µL/min. The mass spectrometer was operated in positive electrospray ionization mode. The spray voltage was 4100 V, the ion transfer tube lens temperature was 325 °C, and the vaporizer temperature was 300 °C. The UPLC fluid was nebulized using N_2 as the sheath gas at a flow rate of 40 unit and the auxiliary gas at a flow rate of 20 unit.

2.6 Quantitation of CCK-4 and Its Metabolites

Quantitation of CCK-4 and its metabolites at each sampling time point was based on the integration of peaks on their chromatograms. The percent of metabolite formation was calculated and converted to the percent of initial parent concentration.

3. RESULTS AND DISCUSSION

3.1 CCK-4 Metabolism in HLMs, MyLMs, RLMs, and MsLMs

Microsomal samples (n = 3) containing 0.05, 0.1, 0.25, 0.5, 1.0, 1.5, and 2.0 mg/mL of microsomal protein were exposed to 5 µM CCK-4 for 60 min. In all species, CCK-4 was extensively metabolized. Under the same incubation conditions, the loss of CCK-4 was found to be more rapid in RLM incubations. No degradation of CCK-4 occurred from incubation with boiled microsomes. An increase in protein concentration resulted in increased degradation of CCK-4.

Figure 1 shows the enzymatic degradation profiles of CCK-4 as a function of protein loading and time. With appropriate protein loading, enzymatic degradation of CCK-4 followed apparent first-order kinetics. The degradation rate constants of CCK-4 at a protein loading of 2.0 mg/mL in HLMs, MyLMs, RLMs, and MsLMs were observed to be 0.0134, 0.0189, 0.0254, and 0.0189 min^{-1}, and half-lives were 51.7, 36.7, 27.3, and 36.7 min, respectively (Figure 2). The intrinsic clearance for HLMs, MyLMs, RLMs, and MsLMs are 6.7, 9.44, 12.69, and 9.44 mL/min/mg, respectively. The half-life of CCK-4 in HLMs was greater than that in MyLMs, RLMs, and MsLMs, which indicates that CCK-4 was metabolically more stable in HLMs.

3.2 Metabolite Profiling

No metabolite formation was detected in the incubations with the negative-control samples. Nine metabolites (M1–M9) of CCK-4 were detected in HLM, MyLM, RLM, and MsLM incubations. Metabolite M1 also existed in the blank matrix, and the M1 concentration increased with the incubation time. Therefore, metabolite M1 could also be an endogenous compound in liver microsomes.

Table 1 shows the exact mass, accurate mass, mass error, and proposed structure for each of the nine metabolites. Metabolites were numbered according to their order of elution from the UPLC column. Metabolite profiles of CCK-4 in HLMs, MyLMs, RLMs, and MsLMs were very similar. All the metabolites detected in these incubations were absent in the negative-control samples.

Quantitation of CCK-4 and its metabolites from HLM, MyLM, RLM, and MsLM incubations are shown in Table 2. It is obvious that HLM, MyLM, RLM, and MsLM incubations exhibited significant differences in the formation of all detected metabolites (Figure 3). In HLM incubations, M2, M6, and M8 were the major metabolites, and the percentages of formation were 18.8, 17.5, and 12.7%, respectively. In MyLM incubations, M2, M7, and M8 were the major metabolites, and the percentages of formation were 51.9, 11.4, and 11.0%, respectively. In RLM incubations, M2, M5, and M8 were the major metabolites, and the percentages of formation were 12.0, 44.0, and 15.1%, respectively. In MsLM incubations, M2, M5, and M8 were the major metabolites, and the percentages of formation were 22.0, 10.4, and 17.4%, respectively.

3.3 Characterization of the Major Metabolites

Metabolite identification was based on the accurate mass, the characteristic mass shifts of the molecular ions $[M+H]^+$, and the product ions obtained from the enhanced product ion mass spectrum of each peak as compared with the CCK-4 standard. The following sections detail the mass spectra of the CCK-4 standard and its metabolites, and the data are interpreted.

3.3.1 UPLC–HRMS Analysis of CCK-4 Standard

The CCK-4 standard was analyzed using UPLC–HRMS, and its retention time (RT) was 17.11 min (Figure 4, top) The fragmentation pattern of CCK-4 was studied to facilitate the interpretation of the mass spectra of its metabolites. The mass spectra of CCK-4 (Figure 4, bottom) showed a protonated molecular ion at mass-to-charge ratio (*m/z*) of 597.2495. The

product ion spectrum of *m/z* 597 (Figure 5) showed a base peak at *m/z* 580, which was formed by the loss of a hydroxyl group. The product ion spectrum of *m/z* 580 from *m/z* 597 (Figure 6) showed a base peak at *m/z* 536, which was formed by the loss of an amide moiety.

3.3.2 Identification of In Vitro Metabolites of CCK-4

The high-resolution, accurate-mass survey injections were processed by using the workflow-based Thermo Scientific Compound Discoverer software. Metabolites of CCK-4 were detected using a workflow that combined multiple orthogonal detection approaches, including a combinatorial metabolite search with a standard multiple mass defect filter and fragment searching. Compared with the controls, nine metabolites were found in the HLM, MyLM, RLM, and MsLM incubates (Figures 7–10). Metabolite M1 also existed in blank liver microsomes as an endogenous compound. Metabolites M3, M4A, M4B, and M9 were minor metabolites that only accounted for 0.1–3.9% of CCK-4, due to their low abundance. We were not able to obtain the MS/MS mass spectra for these metabolites. Their tentative structures were interpreted and assigned solely upon accurate masses and biotransformation pathways. The structures of metabolites M1, M2, M5, M6, M7, and M8 were assigned on the basis of their accurate mass and MS/MS mass spectra.

3.3.2.1 Metabolite M1

The RT of M1 was 3.44–3.55 min. The protonated molecular ion of M1 was 205.0790, which is 392 amu less than that of parent CCK-4 (Figure 11). The product ion spectrum of *m/z* 205 showed a base peak of *m/z* 188 that was formed by the loss of amino moiety (Figure 12).

To compare metabolite M1 to tryptophan, a tryptophan standard was prepared at 1 µg/mL in methanol and water (1:1) and run on an LC–MS using the same method that was used for the incubation samples (Figures 13 and 14). Tryptophan has the same RT and MS/MS profile as metabolite M1. M1 was identified as tryptophan, which was formed as a b-ion when the amide bond of C–N cleaved at the tryptophan residue.[9]

3.3.2.2 Metabolite M2

The RT of M2 was 6.71–6.80 min. The protonated molecular ion of M2 was *m/z* 204.1129, which is 393 amu less than that of CCK-4 (Figure 15) and 1 amu less than that of metabolite M1. The product ion spectrum of *m/z* 204 showed a base peak of *m/z* 187, which was formed by the loss of amino moiety (Figure 16). It was suggested that M2 was a c-ion when the amide bond cleaved at the tryptophan residue.

3.3.2.3 Metabolites M4A, M4B, M5, and M7

Metabolites M5 and M7 (Figures 17 and 20, respectively) had protonated molecular ions of *m/z* 336 and 335, respectively. Their molecular ions were 261 and 262 amu less, respectively, than that of CCK-4, which suggests that from the cleavage of the amide bond between Met and Asp, a b-ion formed M5, and a c-ion formed M7.[9] MS/MS data (Figures 18, 19, 21, and 22) provide further evidence to support the proposed structures.

Metabolites M4A and M4B both showed a protonated molecular ion of *m/z* 351 (Figures 23 and 24); however, because of the low abundance, no MS/MS mass spectra were acquired. Based on their accurate mass, we proposed that metabolites M4A and M4B were isomers and were oxidized metabolites of M7.

3.3.2.4 Metabolite M6

Metabolite M6 (Figure 25) had a protonated molecular ion of *m/z* 295, which was 302 amu less than that of CCK-4. The accurate mass suggested a formula of $C_{14}H_{18}N_2O_5$. On the basis of the biotransformation pathway and MS/MS spectra (Figures 26 and 27), we proposed that Metabolite M6 was derived from CCK-4 by hydrolysis, hydrogenation, and deamidation.

3.3.2.5 Metabolites M3 and M8

Metabolite M8 showed a protonated molecular ion of *m/z* 450 (Figure 28), which is 147 amu less than that of the parent compound. This suggests that a peptide bond cleavage at Asp–Phe left a c-ion of Trp–Met–Asp–NH_2. The MS/MS spectra of M8 (Figures 29 and 30) provided additional evidence to support our proposed structure.

Metabolite M3 showed a protonated molecular ion of *m/z* 466 (Figure 31). Due to the low abundance, no MS/MS spectra were acquired. However, based on the accurate mass, we proposed that metabolite M3 was an oxidized metabolite of M8.

3.3.2.6 Metabolite M9

Metabolite M9 showed a protonated molecular ion of *m/z* 598 (Figure 32). As was true for metabolites M4A, M4B, and M3, due to the low abundance of metabolite M9, no MS/MS spectra could be acquired. Based on its accurate mass, we proposed that metabolite M9 was a deamidation product of CCK-4.

3.3.2.7 Biotransformation Pathway of CCK-4

The biotransformation pathways of CCK-4 in HLM, MyLM, RLM, and MsLM incubations are proposed based on the metabolites identified in this study (Figure 33). Metabolites M1 and M2 were formed by peptide bond cleavage at Trp–Met, metabolite M1 was a b-ion, and metabolite M2 was a c-ion. Similarly, the peptide bond cleavage at Met–Asp formed metabolites M5 and M7. Metabolites M4A and M4B were formed by single oxidation of metabolite M7. Peptide bond cleavage at Asp–Phe formed metabolite M8, and single oxidation of M8 formed metabolite M3. CCK-4 went through complex hydrolysis, hydrogenation, and deamidation to form metabolite M6, and metabolite M9 was formed by deamidation of CCK-4.

Table 1. Summary of CCK-4 and Its Major Metabolites
in HLM, MyLM, RLM, and MsLM Incubations

CCK-4 and Metabolites	Exact Mass	Accurate Mass	Mass Error (ppm)	RT (min)	Structure
CCK-4	597.2490	597.2495	–0.84	17.11	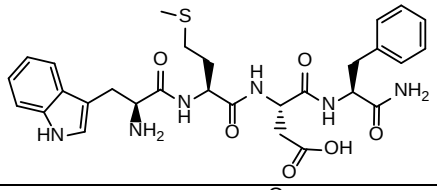
M1	205.0972	205.0970	0.98	3.44–3.55	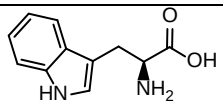
M2	204.1131	204.1129	0.98	6.71–6.80	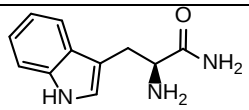
M3	466.1755	466.1755	0.00	8.82	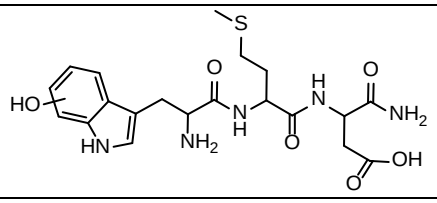
M4A and M4B	351.1485	351.1484	0.28	9.07–9.12 9.31–9.35	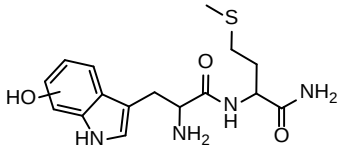
M5	336.1375	336.1375	0.00	10.39–10.44	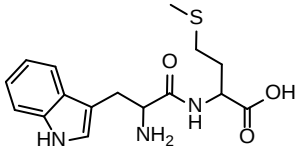
M6	295.1288	295.1286	0.68	10.91–10.95	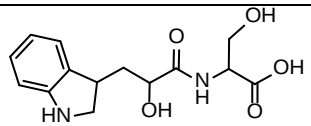
M7	335.1536	335.1535	0.30	11.78–11.80	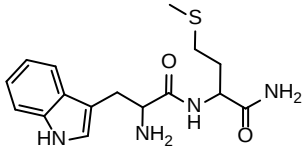
M8	450.1806	450.1806	0.00	12.63–12.64	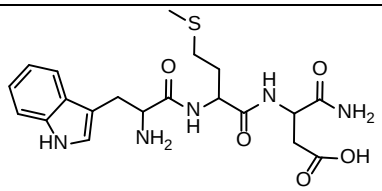
M9	598.2330	598.2335	–0.84	16.56–16.58	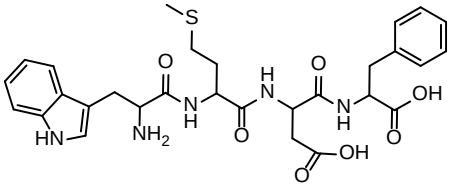

Table 2. Quantitation of CCK-4 and Its Metabolites in HLM, MyLM, RLM, and MsLM Incubations

Liver Microsomes	Time Point (min)	Amount of CCK-4 at 0 min (%)										
		M1	**M2**	**M3**	**M4A**	**M4B**	**M5**	**M6**	**M7**	**M8**	**M9**	**CCK-4**
HLM (2.0 mg/mL)	0–2	4.66	0.00	0.00	0.00	0.00	0.00	24.86	0.36	0.83	0.29	100.00
	10–20	6.42	0.00	0.50	0.39	0.38	0.44	25.58	8.29	8.48	1.36	81.50
	20–40	8.44	0.00	1.06	0.96	0.95	1.00	17.54	9.45	10.90	1.70	59.86
	40–60	10.68	18.79	1.38	1.54	1.56	1.57	17.51	5.21	12.72	1.76	44.06
MyLM (2.0 mg/mL)	0–2	2.32	0.00	0.00	0.00	0.00	0.00	13.49	0.30	1.21	0.31	100.00
	10–20	4.27	0.00	0.08	0.87	1.06	1.24	13.77	6.15	8.85	0.49	63.94
	20–40	7.11	32.29	0.17	2.42	2.54	3.20	11.87	9.37	10.79	0.50	43.13
	40–60	10.16	51.93	0.25	3.93	4.01	5.20	7.55	11.39	11.07	0.47	29.35
RLM (2.0 mg/mL)	0–2	1.83	0.00	0.00	0.00	0.00	0.00	5.78	0.39	1.46	0.00	100.00
	10–20	2.55	0.00	0.06	0.35	0.47	2.66	4.46	3.82	10.93	0.55	63.65
	20–40	3.76	0.00	0.14	0.87	1.29	5.94	8.05	4.66	15.94	0.44	42.16
	40–60	5.58	21.98	0.24	1.49	2.53	10.37	5.71	5.74	17.38	0.40	29.40
MsLM (2.0 mg/mL)	0–2	3.00	0.00	0.00	0.00	0.00	0.21	8.46	2.03	1.59	1.02	100.00
	10–20	5.81	0.00	0.06	0.43	0.66	18.79	7.66	12.66	8.83	1.34	59.47
	20–40	9.90	0.00	0.10	0.87	1.43	34.62	6.86	12.88	12.25	1.02	35.70
	40–60	13.89	11.95	0.14	1.22	2.22	43.97	5.88	3.59	15.11	0.76	22.26

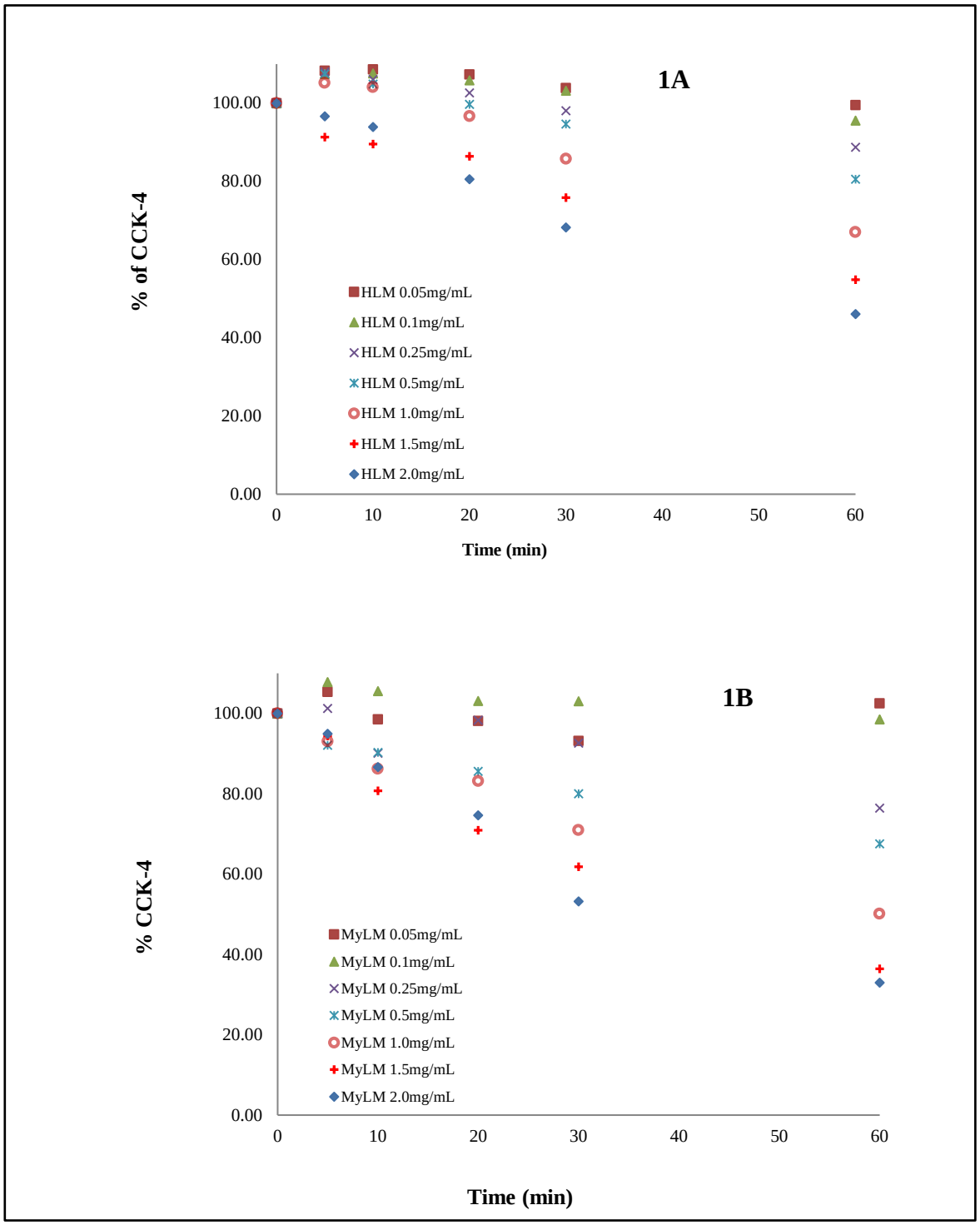

(continued)

Figure 1. The decrease of CCK-4 as a function of protein loading and incubation time by (1A) HLMs, (1B) MyLMs, (1C) RLMs, and (1D) MsLMs. Values are means of triplicate studies.

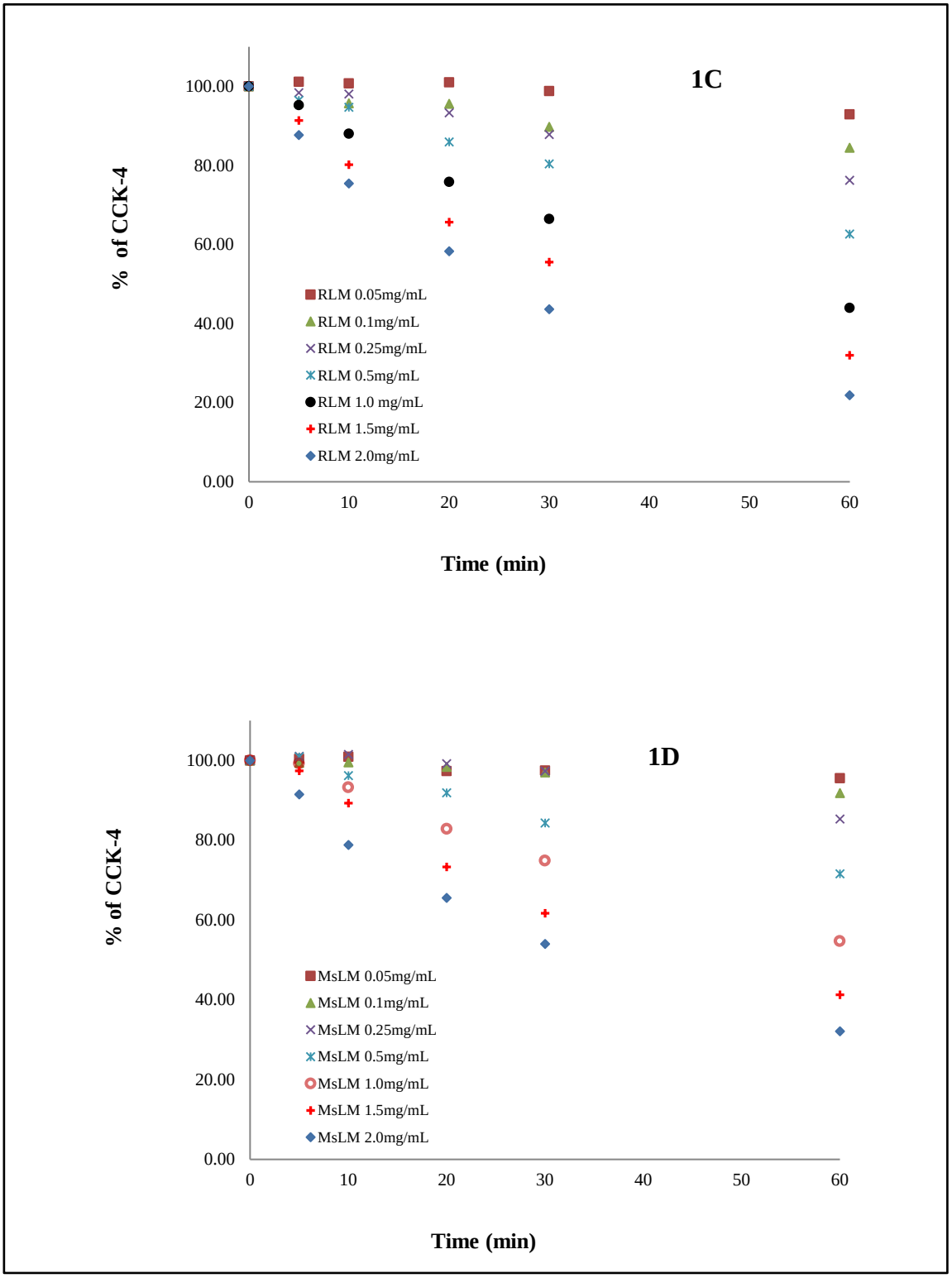

Figure 1 (continued). The decrease of CCK-4 as a function of protein loading and incubation time by (1A) HLMs, (1B) MyLMs, (1C) RLMs, and (1D) MsLMs.
Values are means of triplicate studies.

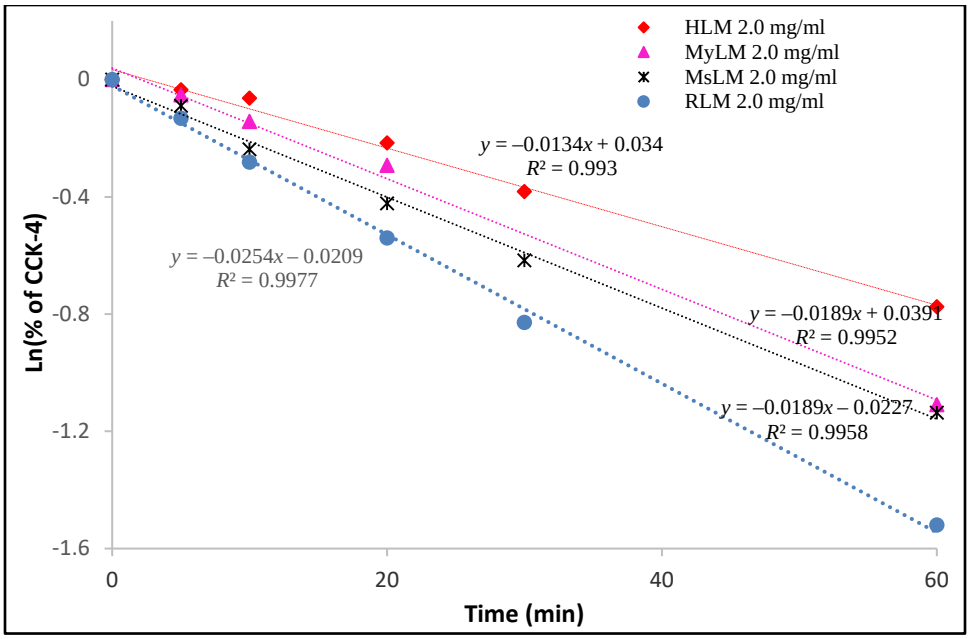

Figure 2. Metabolic degradation kinetics of CCK-4 in HLM, MyLM, RLM, and MsLM incubations. Values are means of triplicate studies.

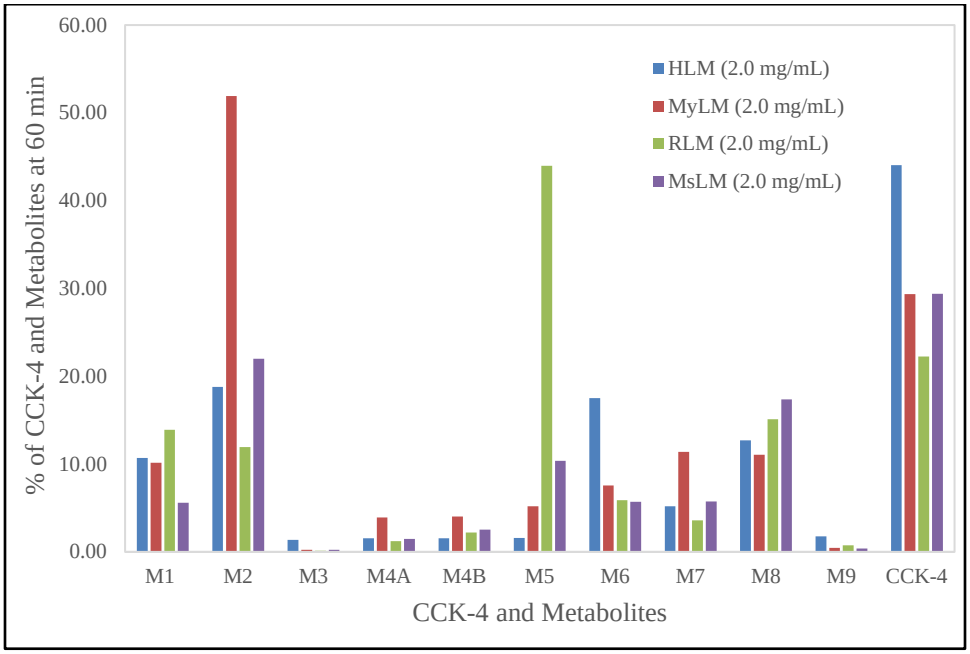

Figure 3. Interspecies comparison of liver microsome contributions to the metabolism of CCK-4 (relative concentration of metabolites vs mean CCK-4 after 60 min incubation in HLMs, MyLMs, RLMs, and MsLMs).

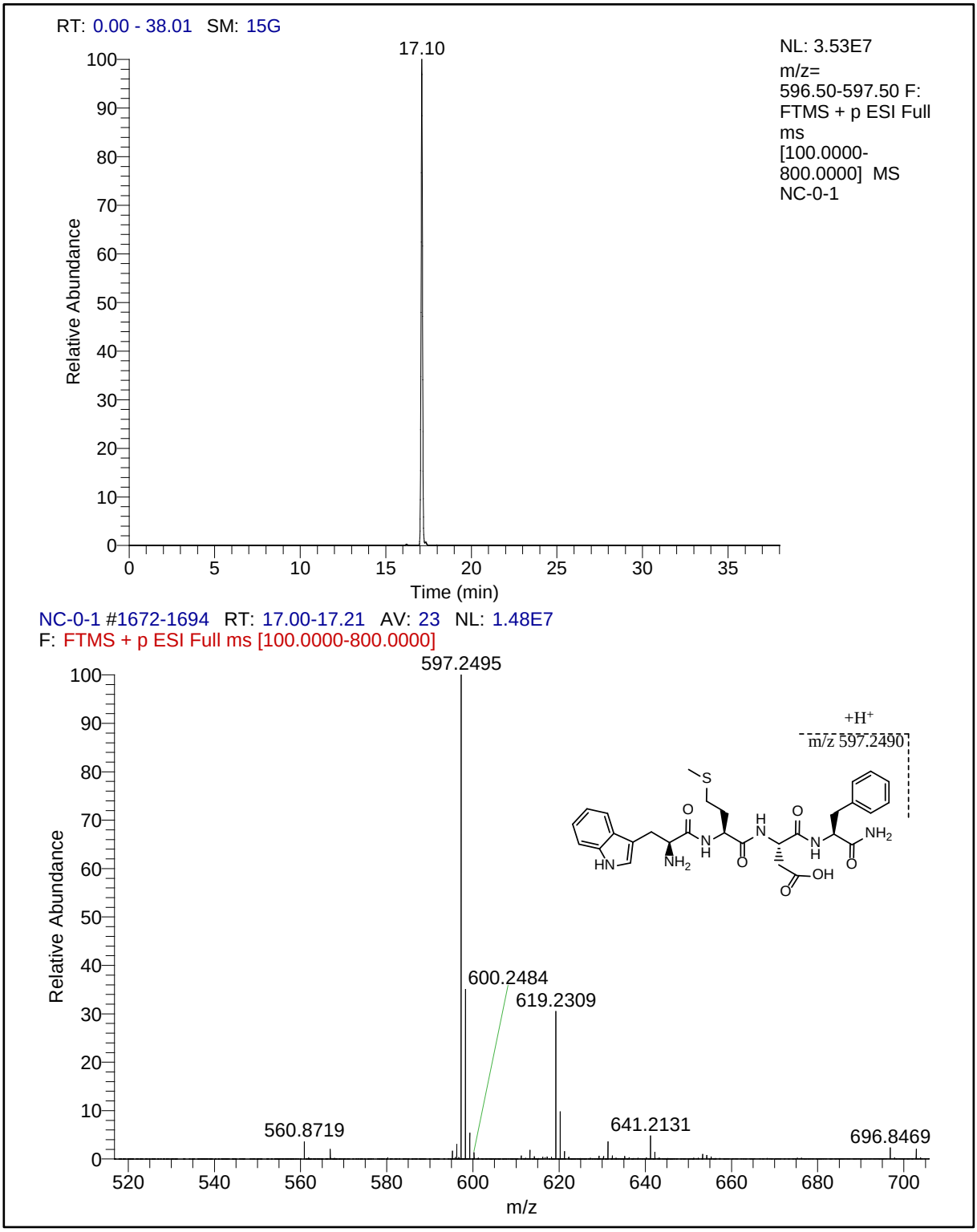

Figure 4. UPLC RT extracted ion chromatogram(EIC): (top) and mass spectrum of CCK-4 standard (bottom) showed a protonated molecular ion at *m/z* 597.

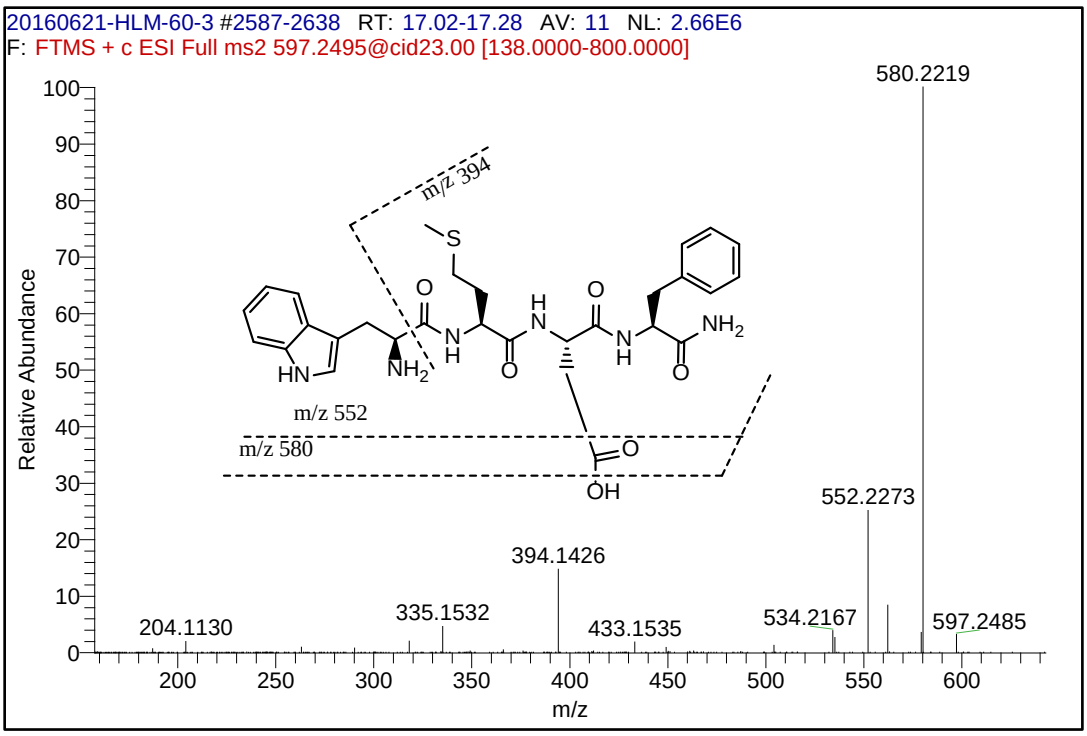

Figure 5. The product ion spectrum of *m/z* 597 (CCK-4) standard and proposed fragments.

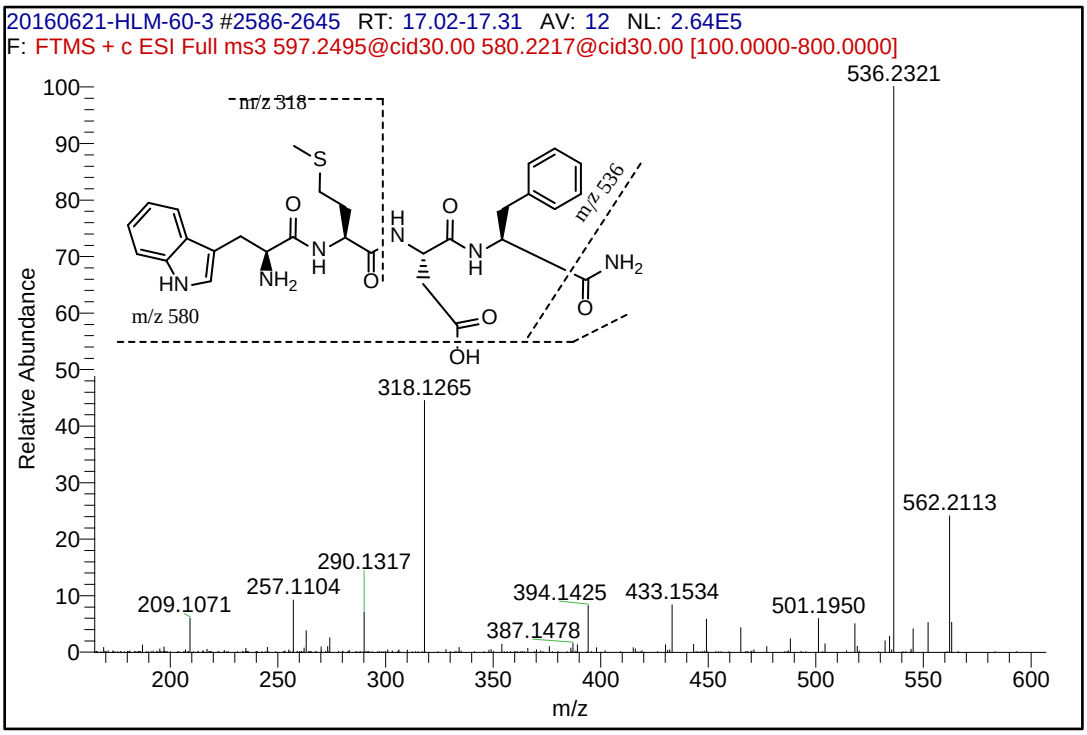

Figure 6. The product ion spectrum of *m/z* 580 from *m/z* 597 and proposed fragments.

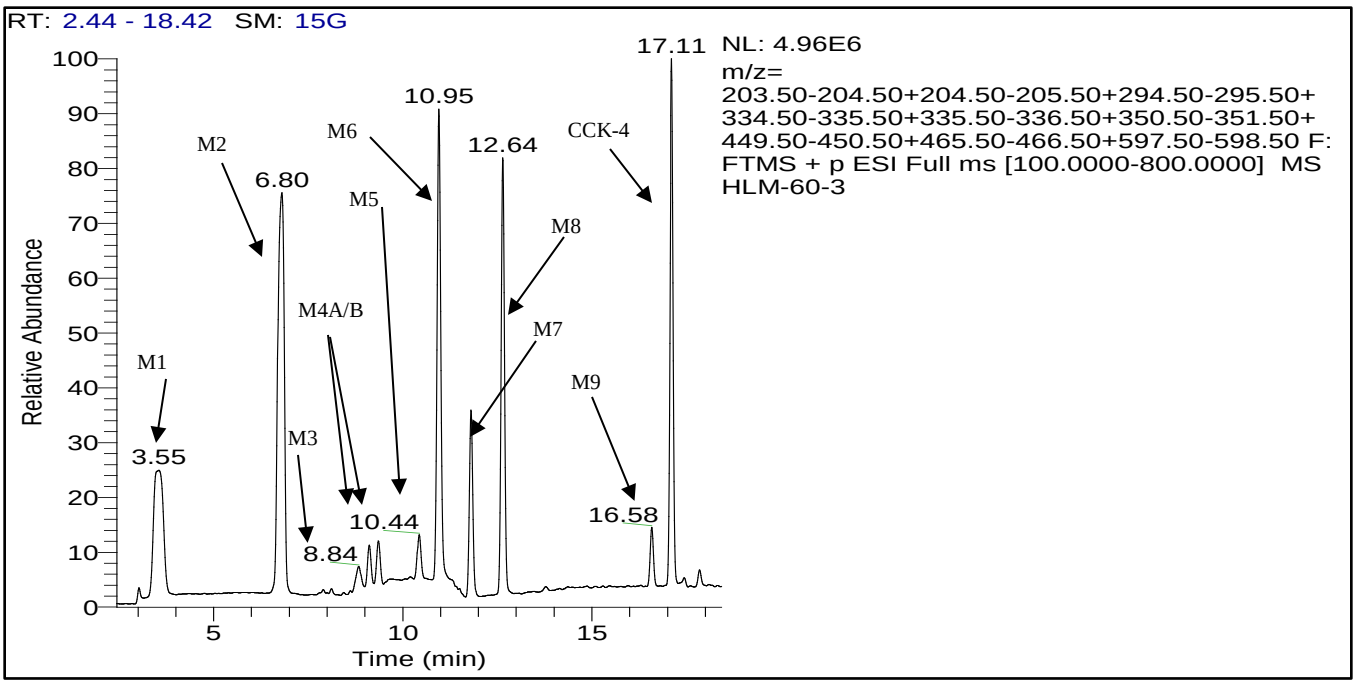

Figure 7. EIC of CCK-4 and its meabolites in 2.0 mg/mL HLM incubation for 60 min.

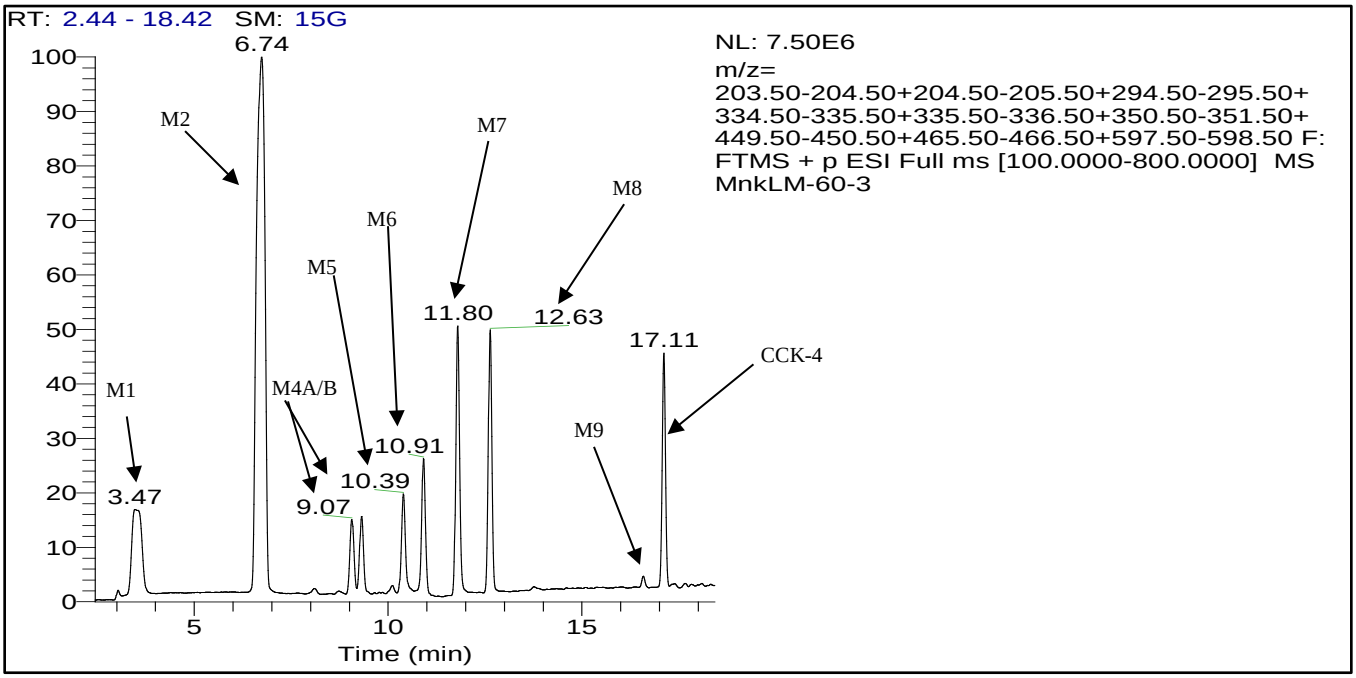

Figure 8. EIC of CCK-4 and its metabolites in 2.0 mg/mL MyLM incubation for 20 min.

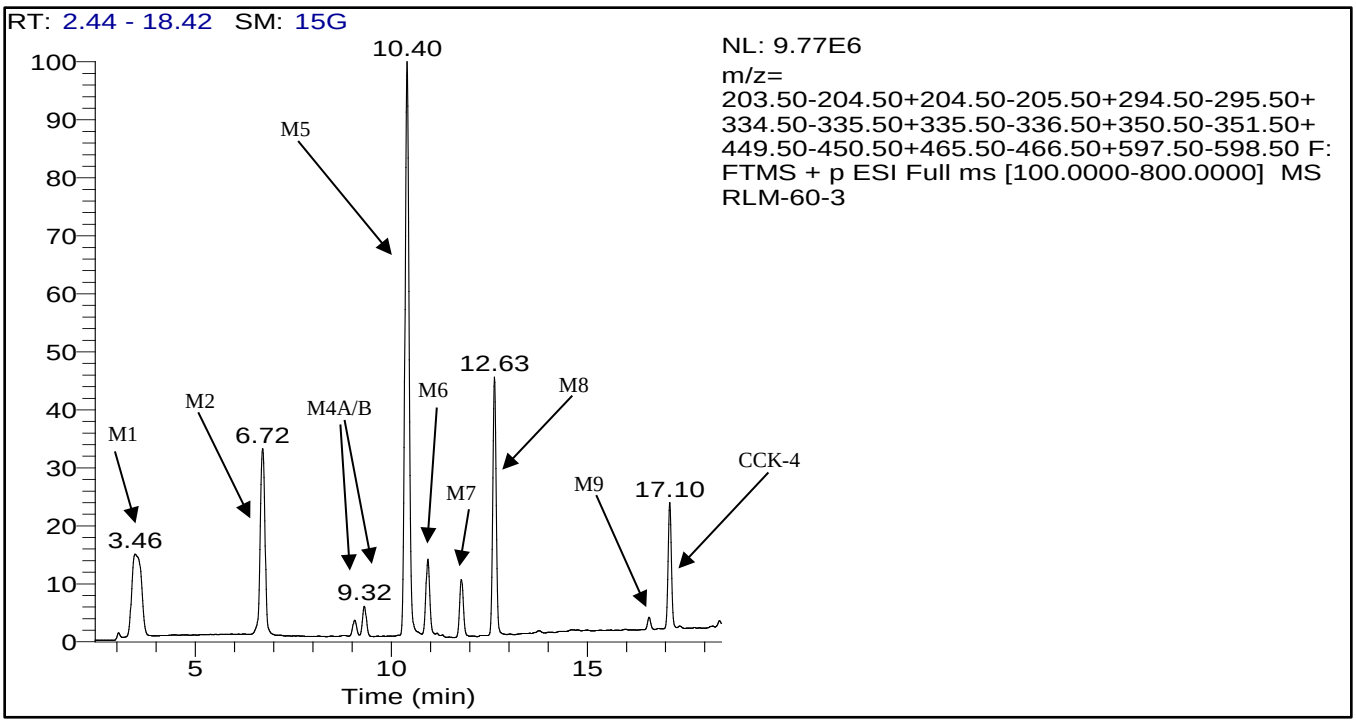

Figure 9. EIC of CCK-4 and its metabolites in 2.0 mg/mL RLM incubation for 30 min.

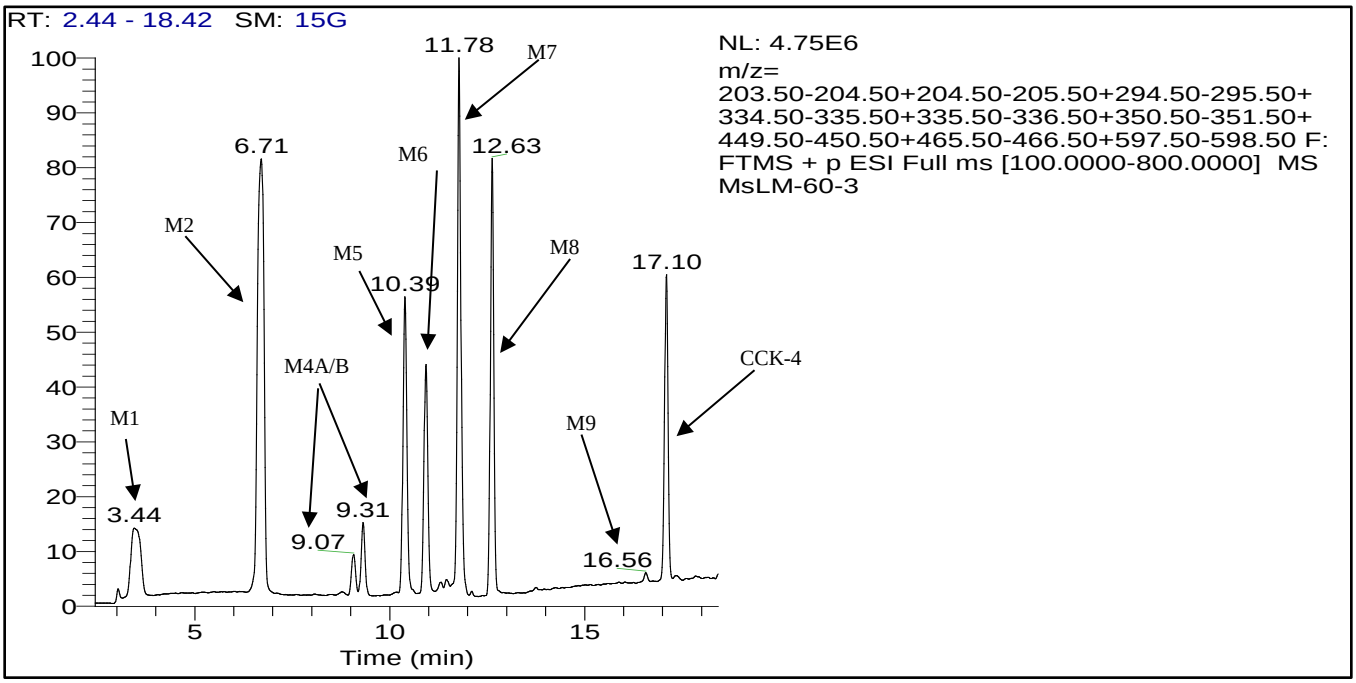

Figure 10. EIC of CCK-4 and its metabolites in 2.0 mg/mL MsLM incubation for 20 min.

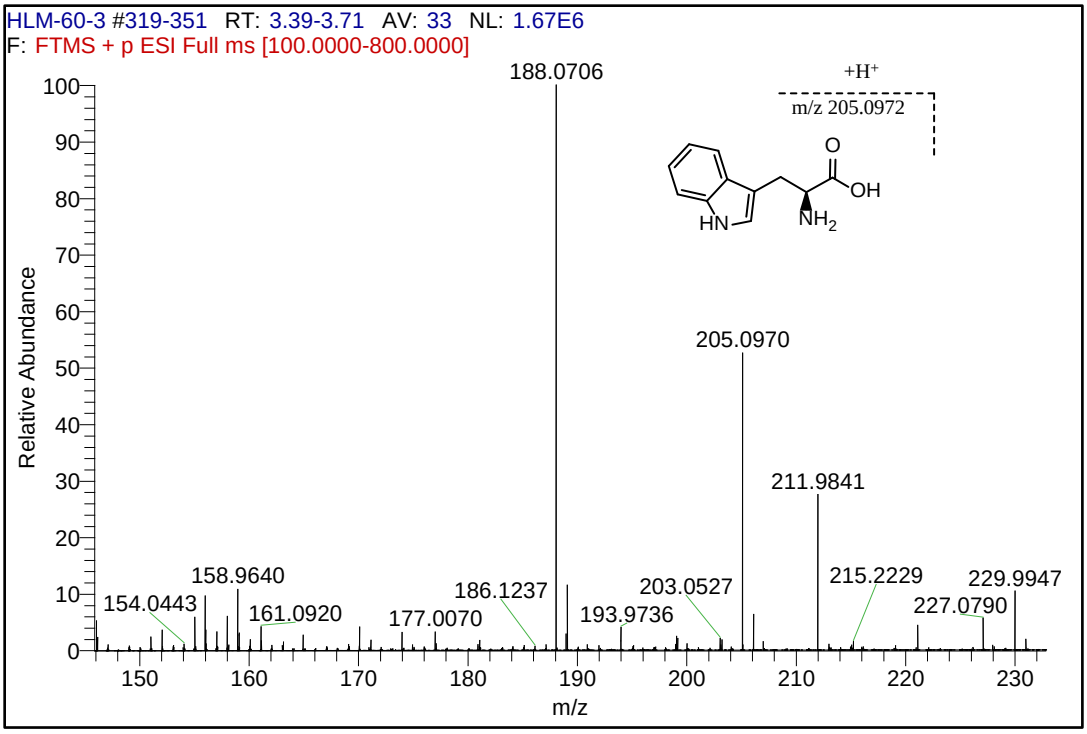

Figure 11. Metabolite M1 (RT 3.44–3.55 min) protonated molecular ion at *m/z* 205.

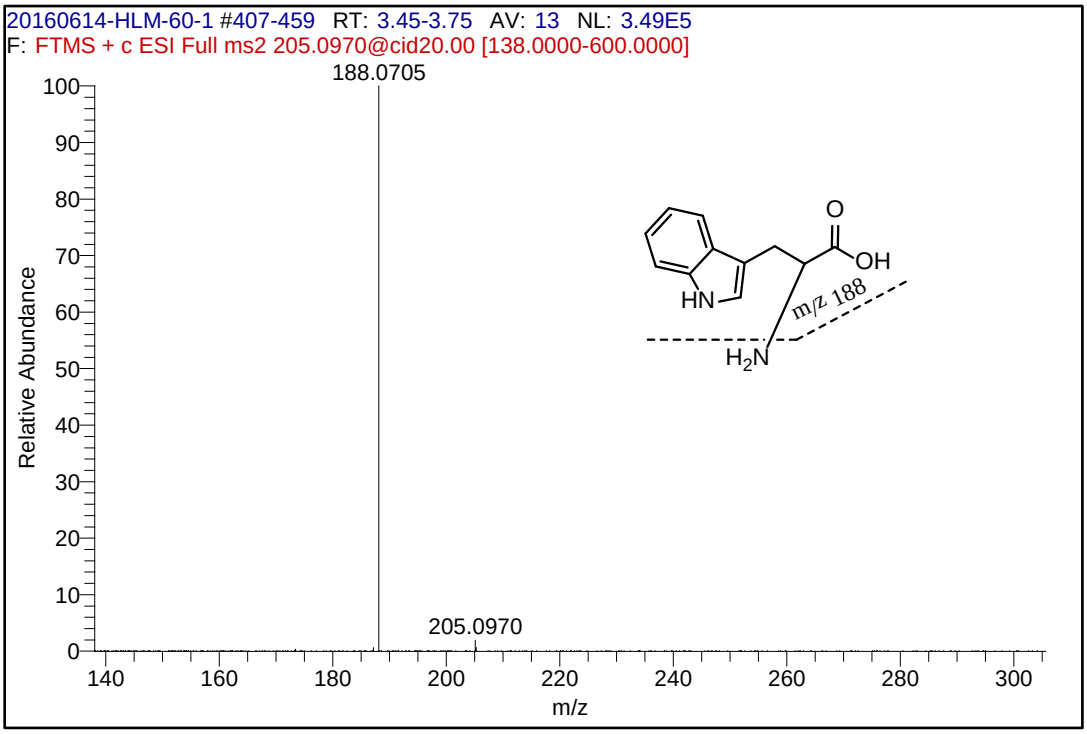

Figure 12. The product ion spectrum of *m/z* 205 (metabolite M1) and proposed fragments.

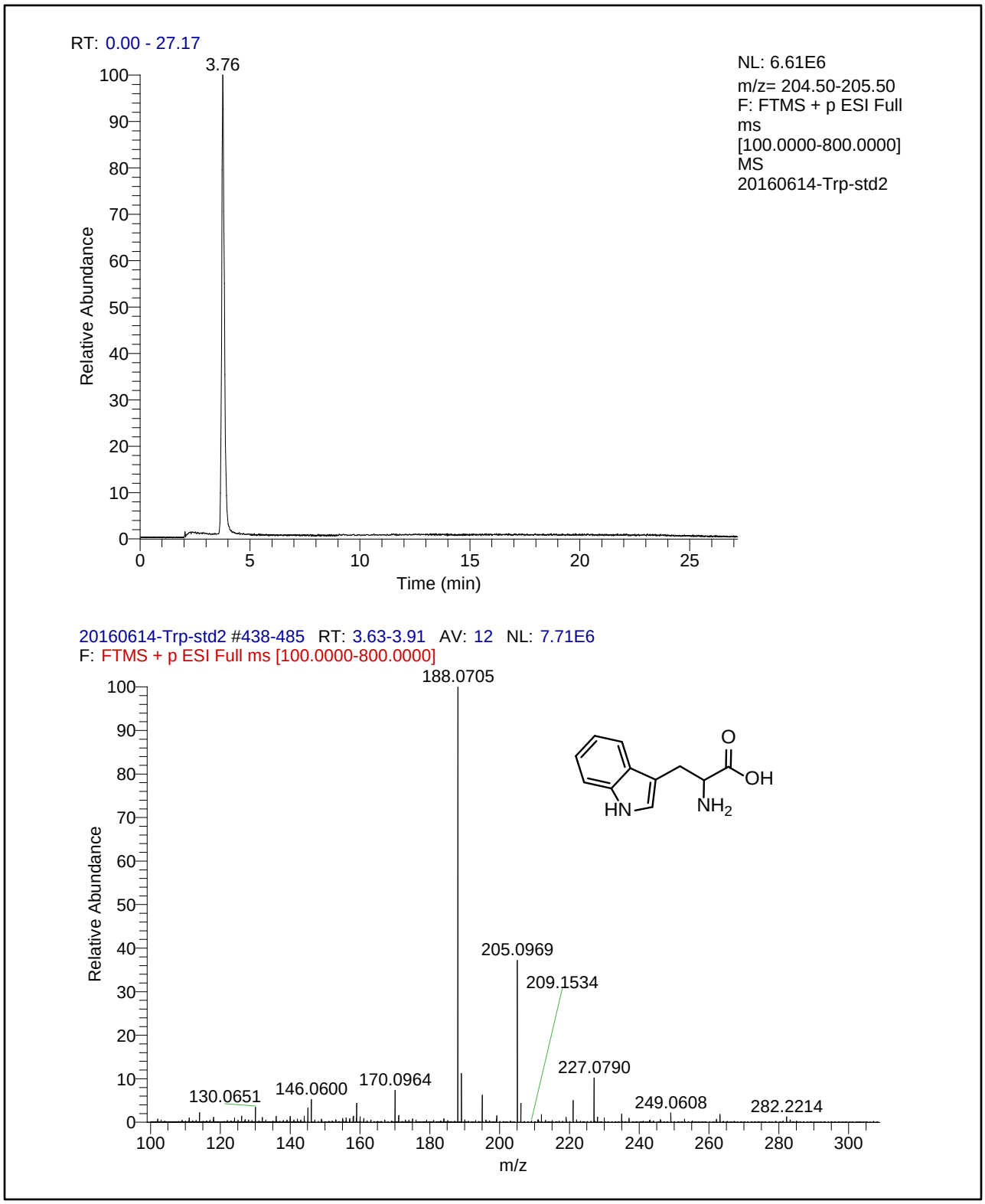

Figure 13. UPLC RT (top) and mass spectrum of tryptophan standard (bottom) showed a protonated molecular ion at *m/z* 205.

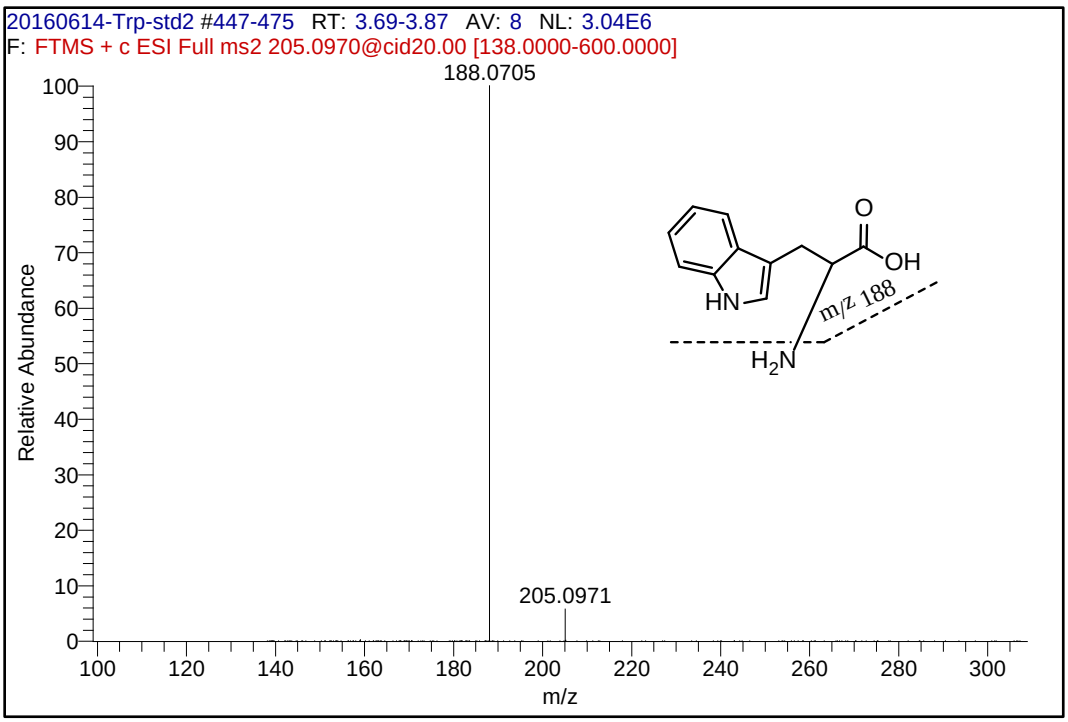

Figure 14. The product ion spectrum of tryptophan standard (*m/z* 205) and proposed fragments.

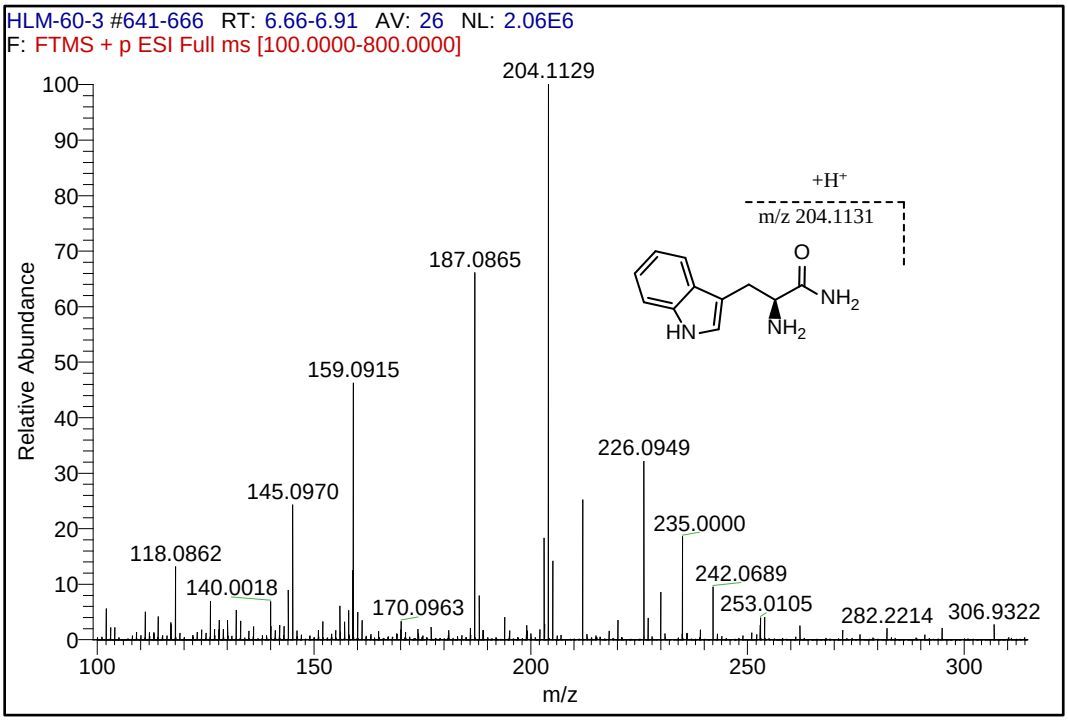

Figure 15. Metabolite M2 (RT 6.71–6.80 min) protonated molecular ion at *m/z* 204.

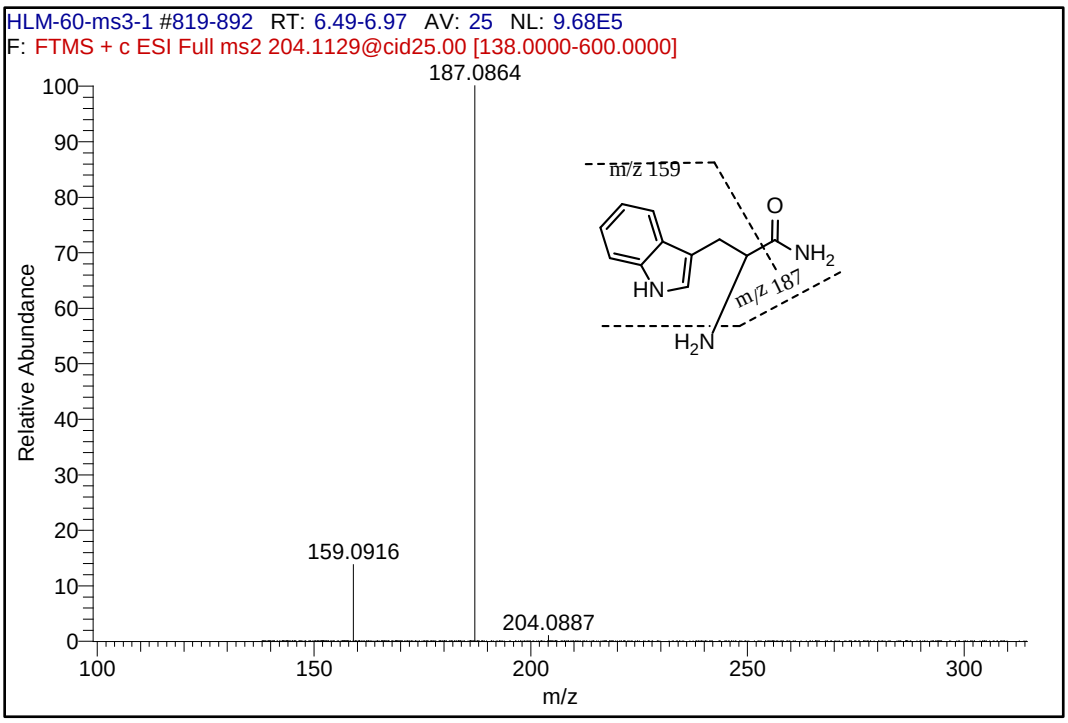

Figure 16. The product ion spectrum of *m/z* 204 (metabolite M2) and proposed fragments.

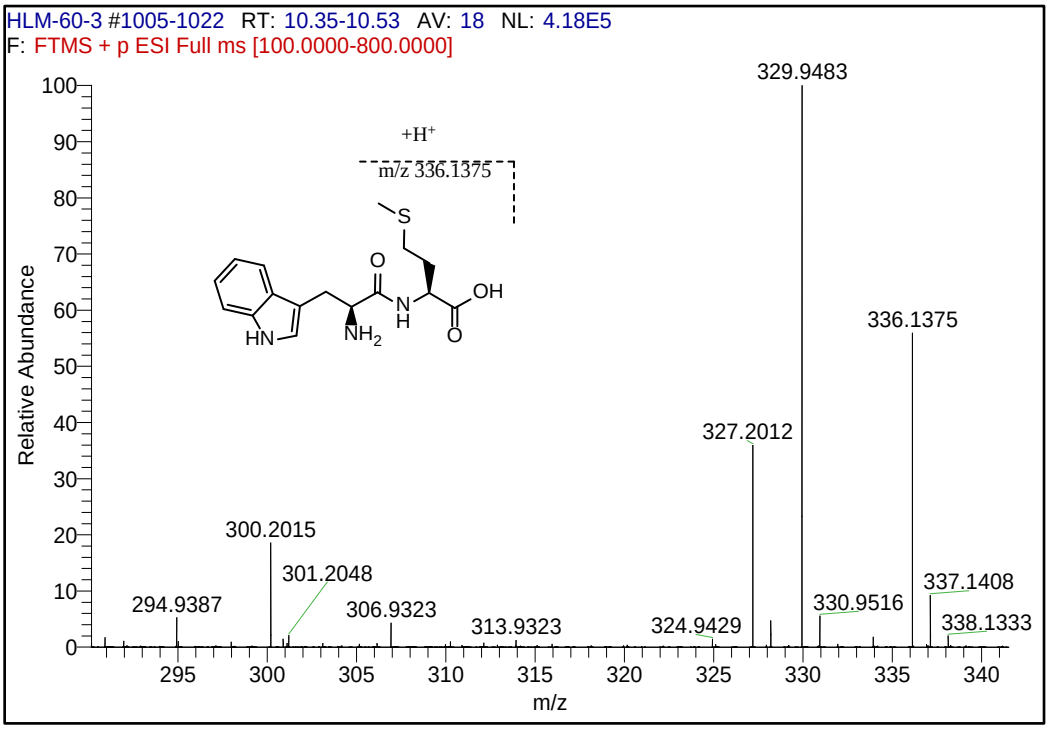

Figure 17. Metabolite M5 (RT 10.39–10.44 min) protonated molecular ion at *m/z* 336.

.

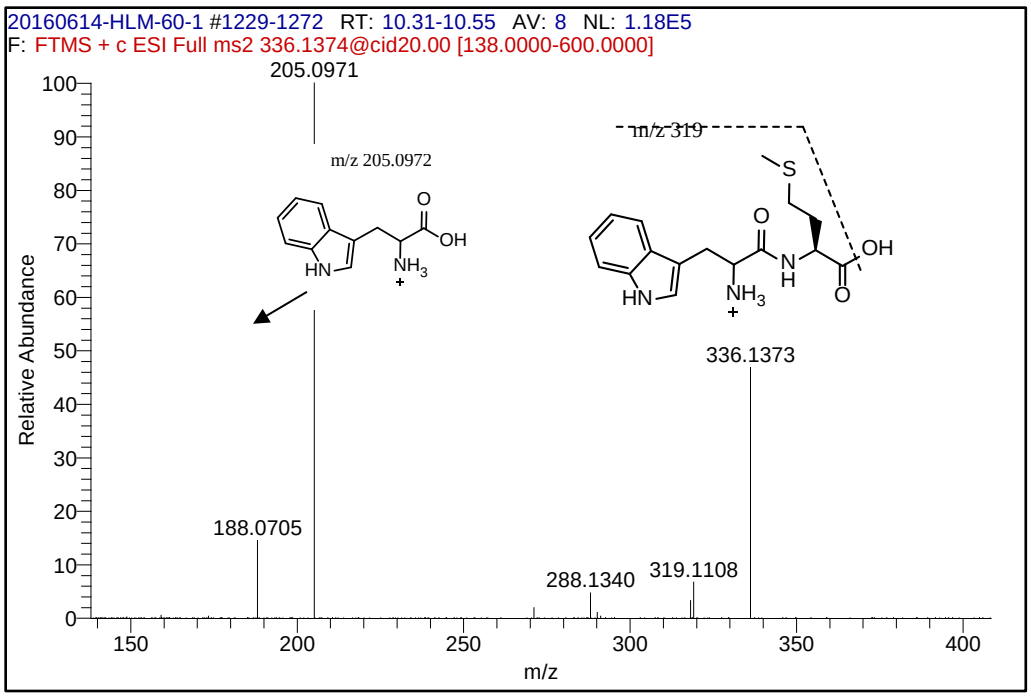

Figure 18. The product ion spectrum of *m/z* 336 (metabolite M5) and proposed fragments.

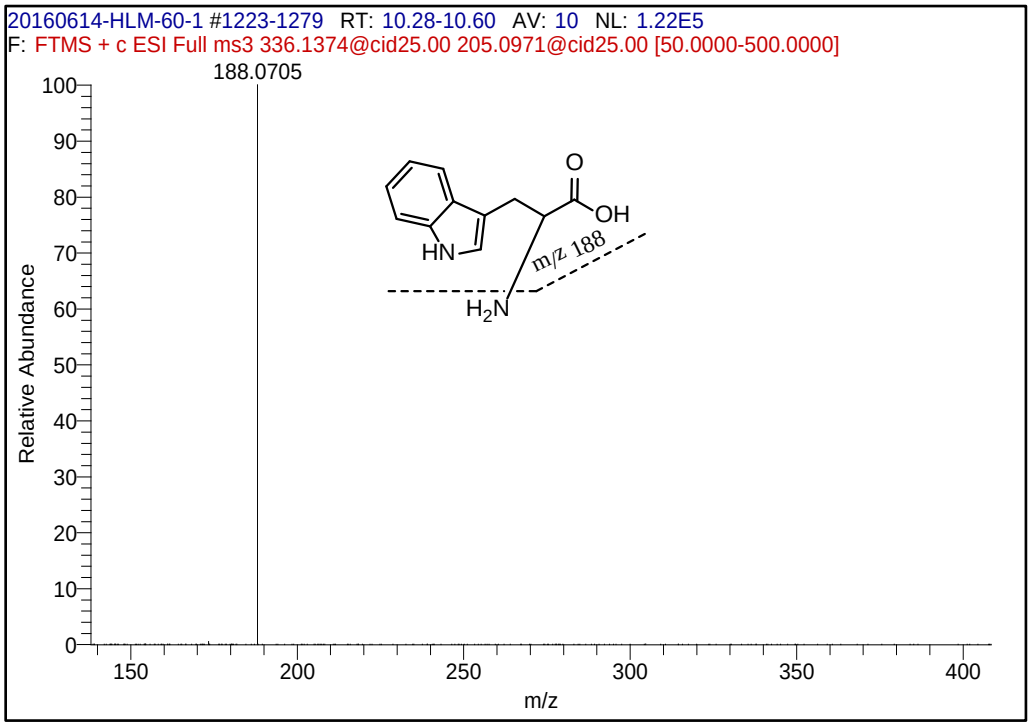

Figure 19. The product ion spectrum of *m/z* 205 from metabolite M5 and proposed fragments.

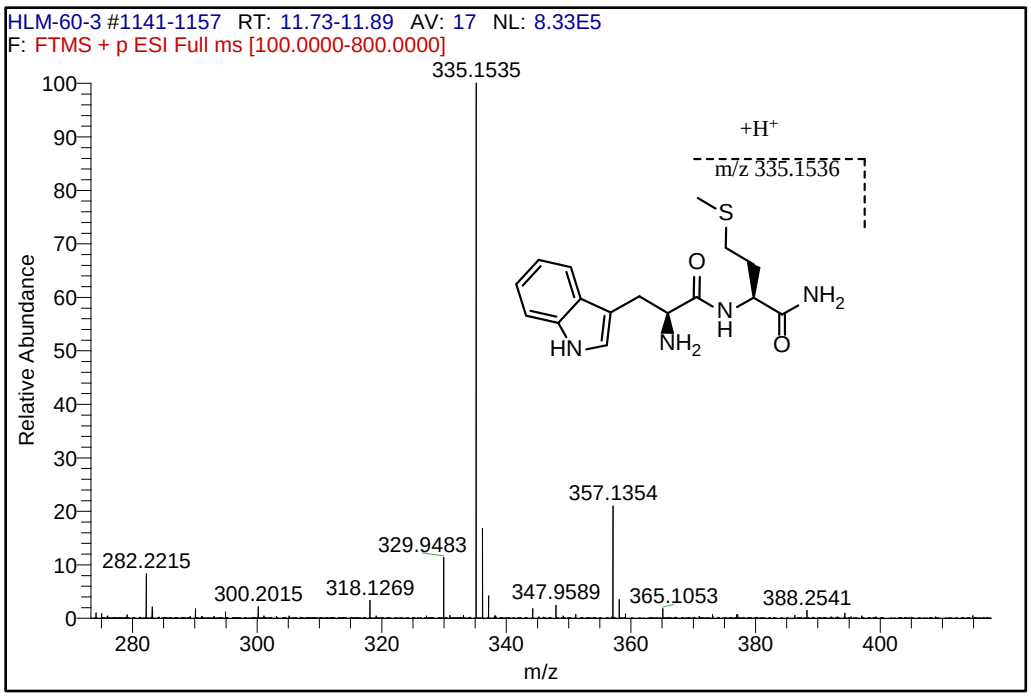

Figure 20. Metabolite M7 (RT 11.78–11.80 min) protonated molecular ion at *m/z* 335.

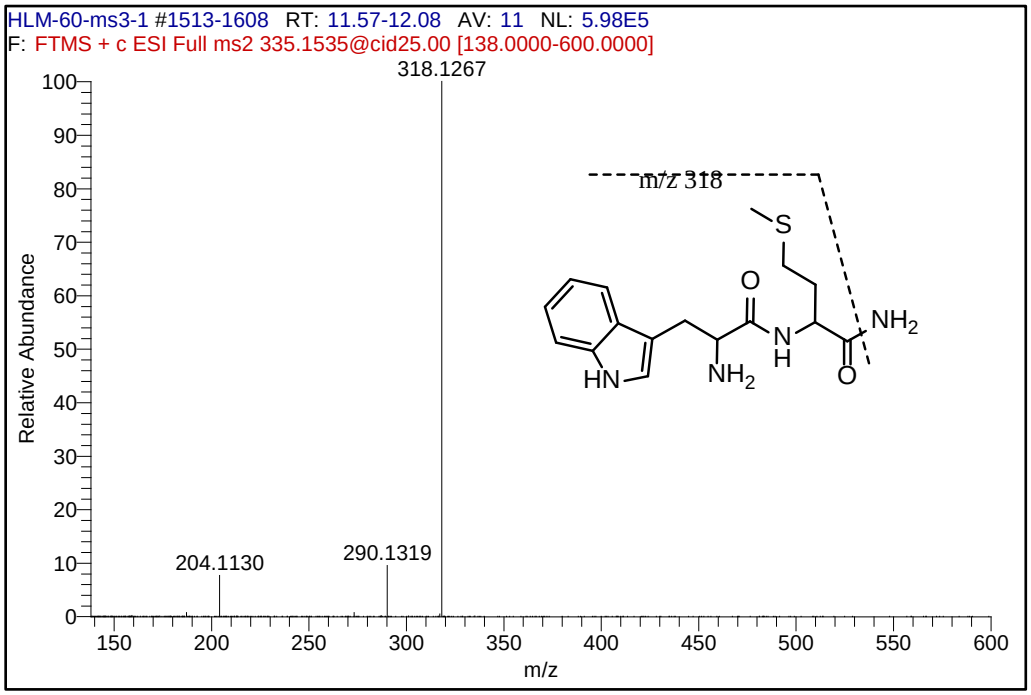

Figure 21. The product ion spectrum of *m/z* 335 (metabolite M7) and proposed fragments.

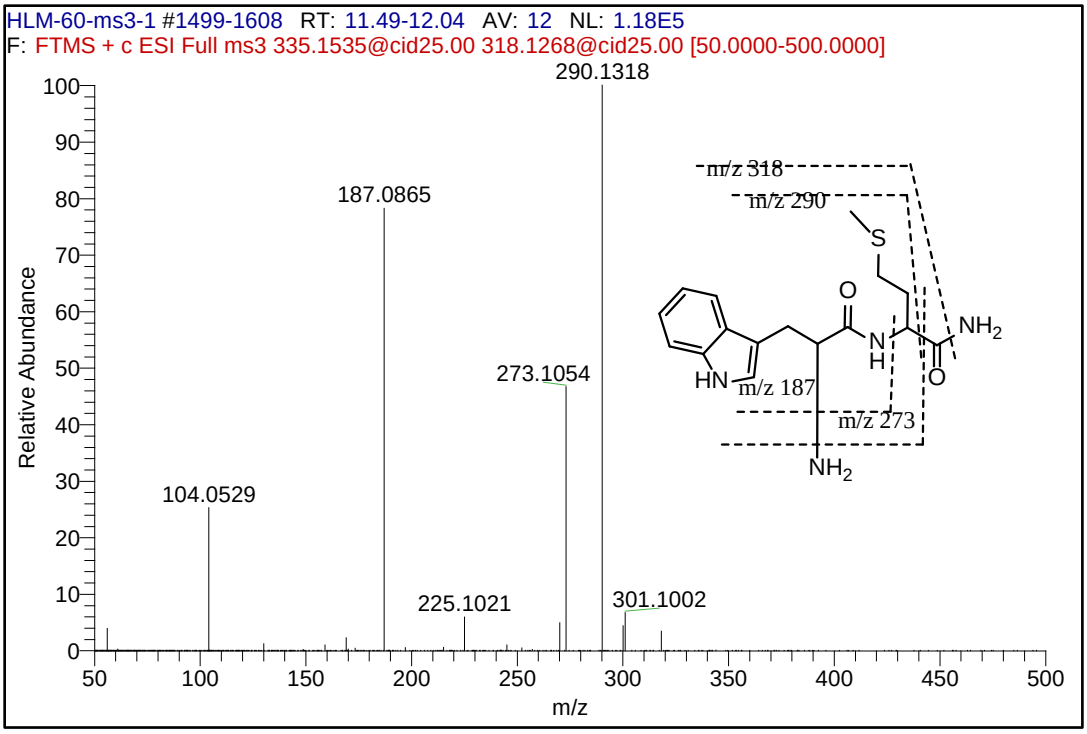

Figure 22. The product ion spectrum of *m/z* 318 from metabolite M7 and proposed fragments.

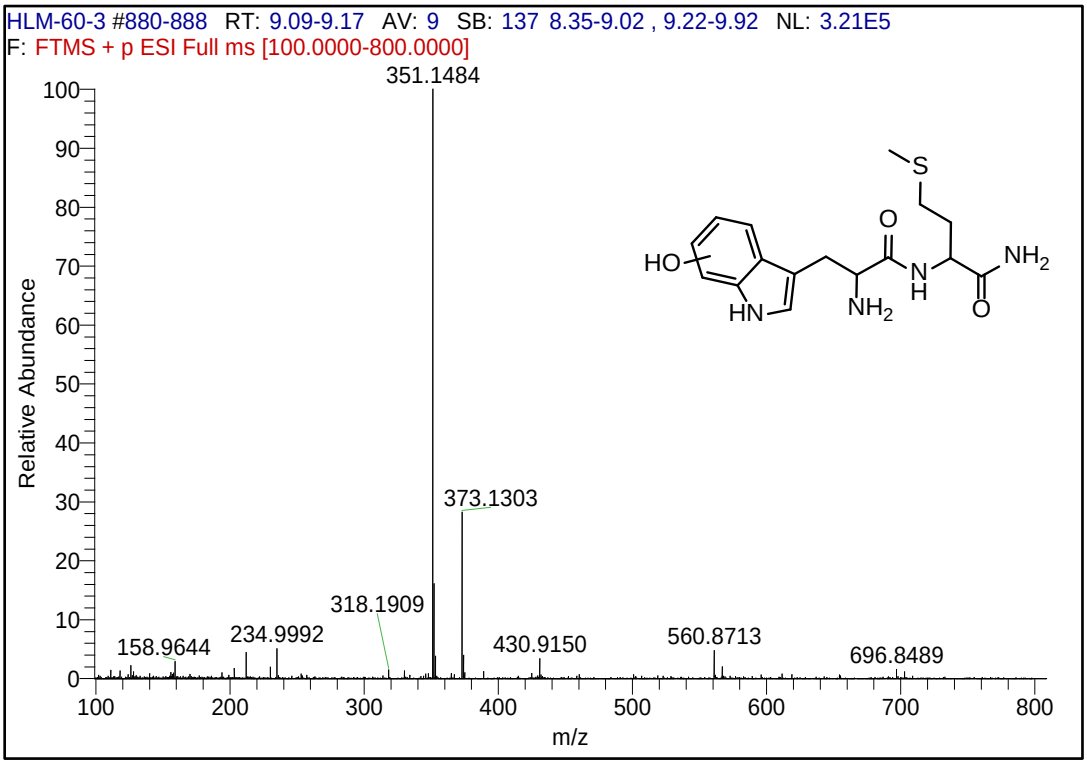

Figure 23. Metabolite M4A (RT 9.07–9.12 min) protonated molecular ion at *m/z* 351.

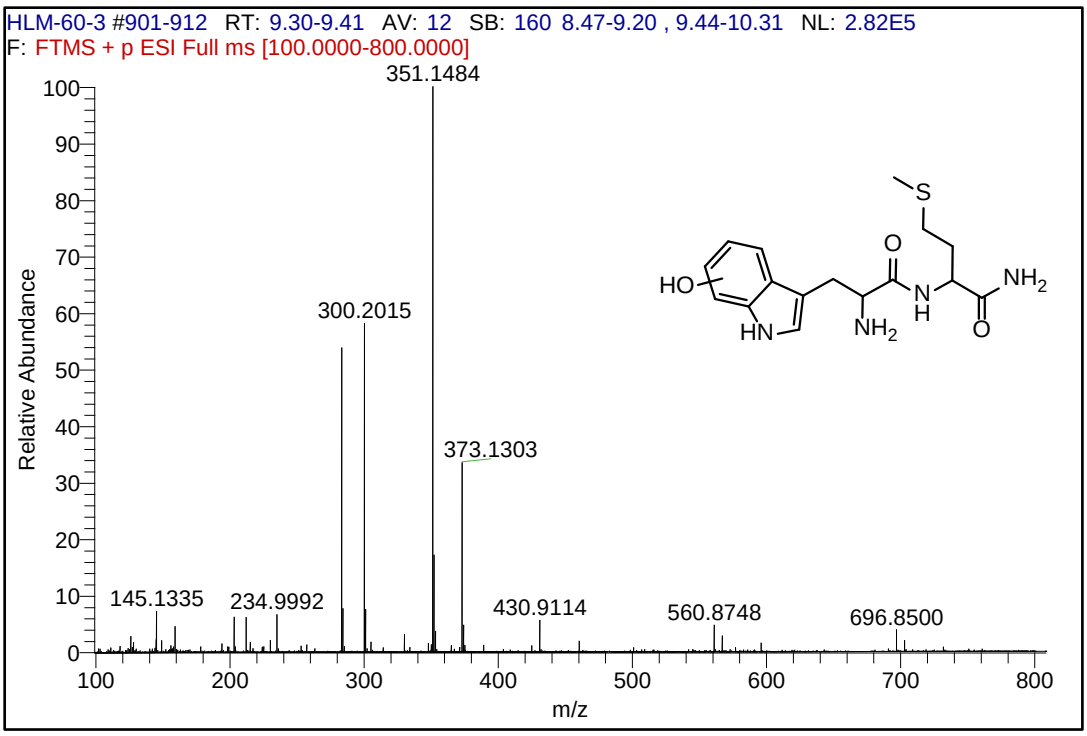

Figure 24. Metabolite M4B (RT 9.31–9.35 min) protonated molecular ion at *m/z* 351.

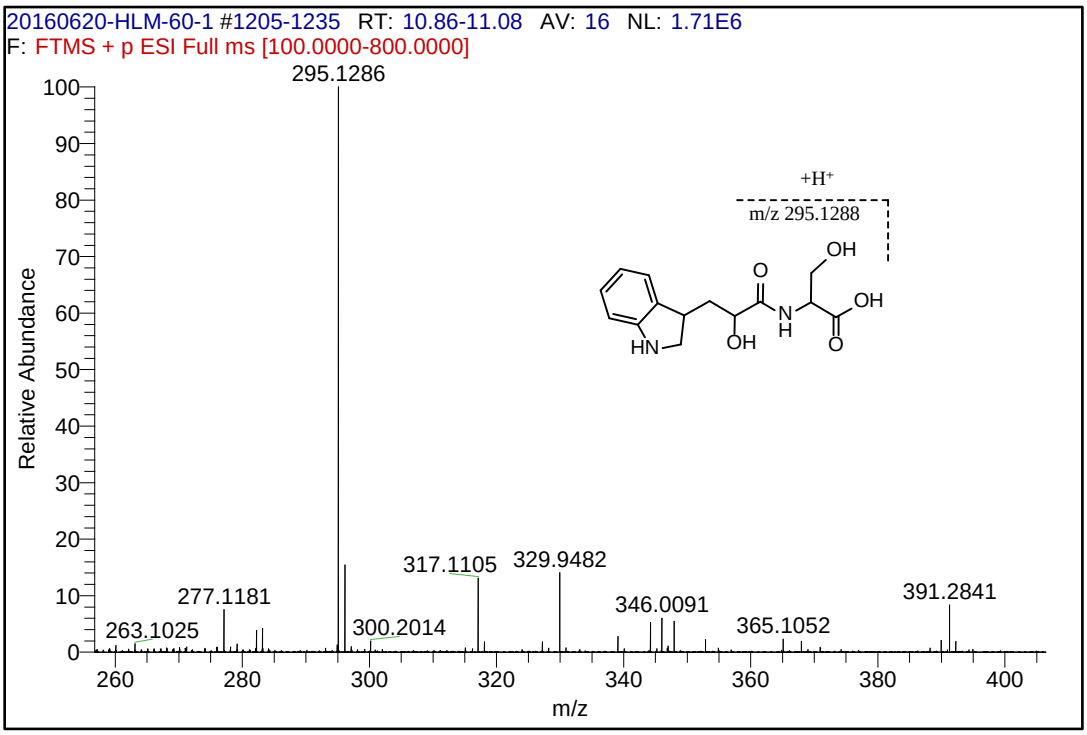

Figure 25. Metabolite M6 (RT 10.91–10.95 min) protonated molecular ion at *m/z* 295.

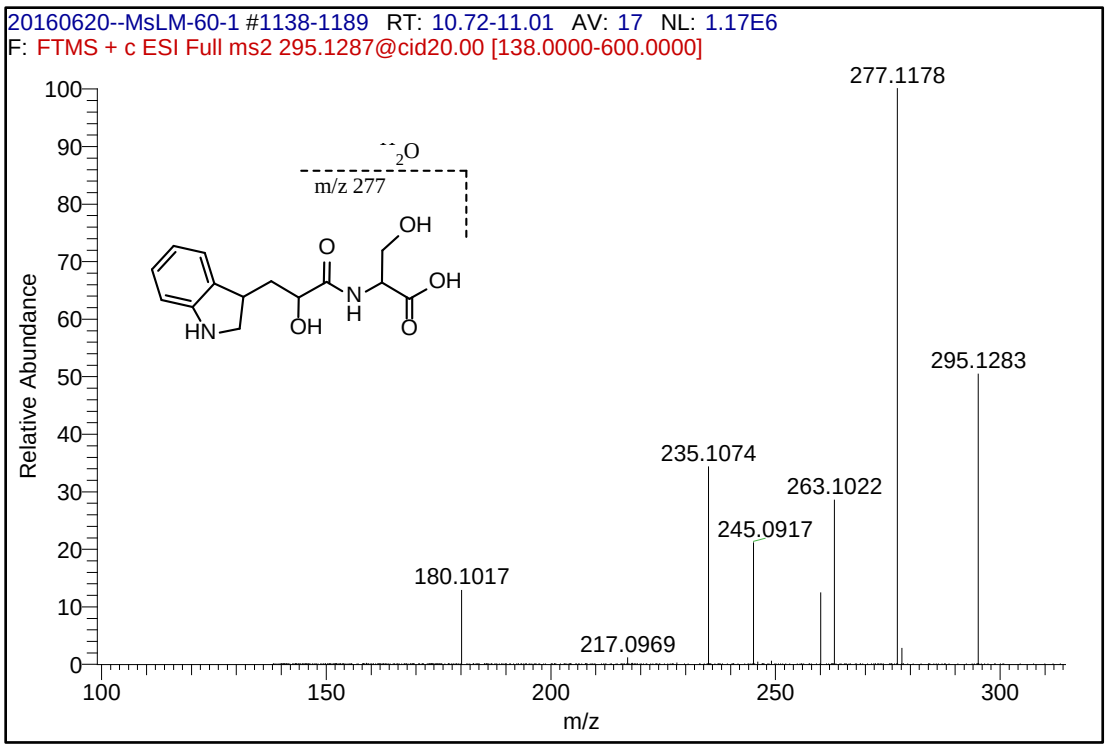

Figure 26. The product ion spectrum of *m/z* 295 (metabolite M6) and proposed fragments.

.

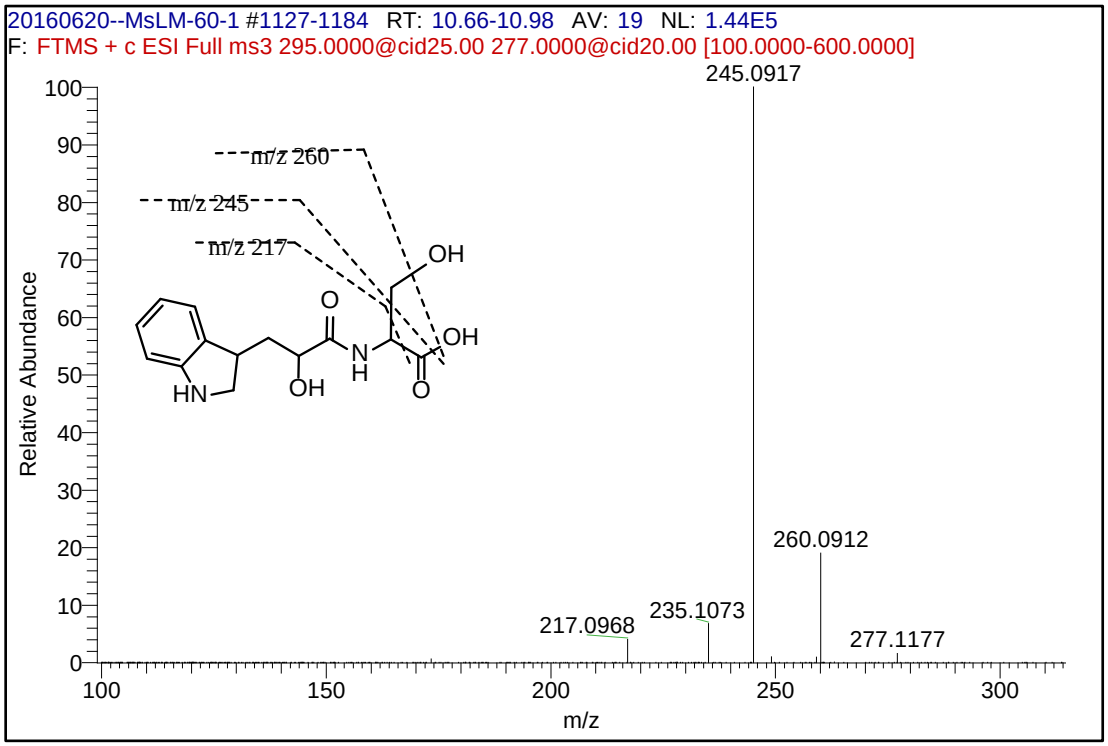

Figure 27. The product ion spectrum of *m/z* 277 from metabolite M6 and proposed fragments.

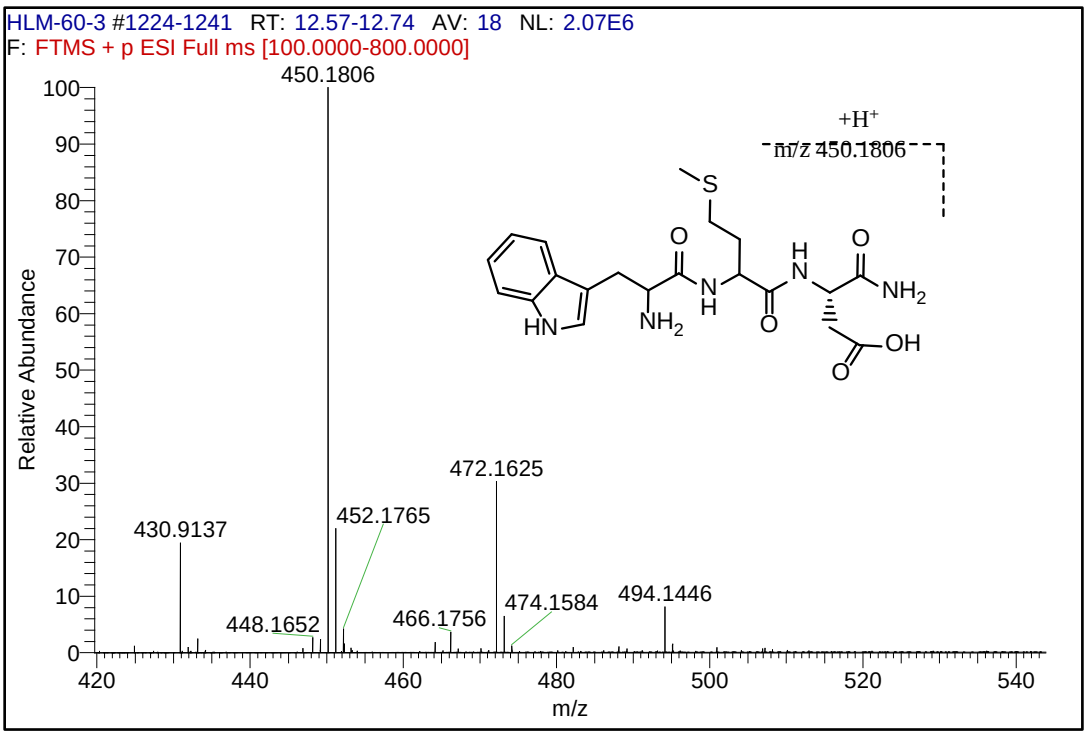

Figure 28. Metabolite M8 (RT 16.12.63–12.64 min) protonated molecular ion at *m/z* 450.

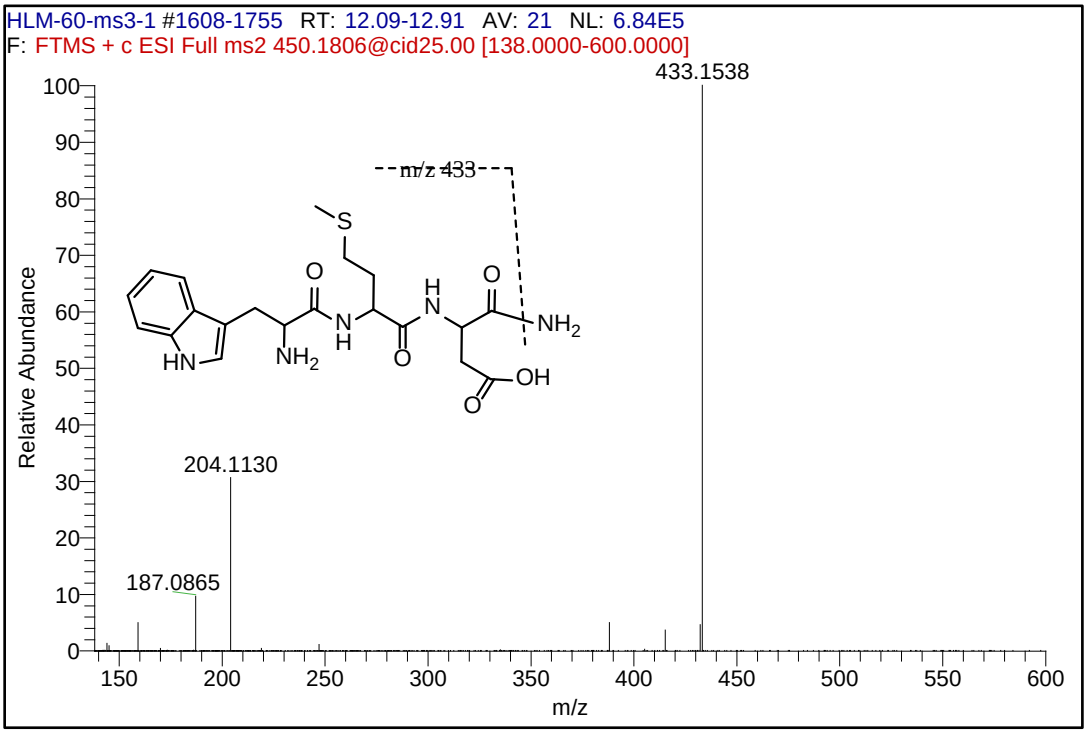

Figure 29. The product ion spectrum of *m/z* 450 (metabolite M8) and proposed fragments.

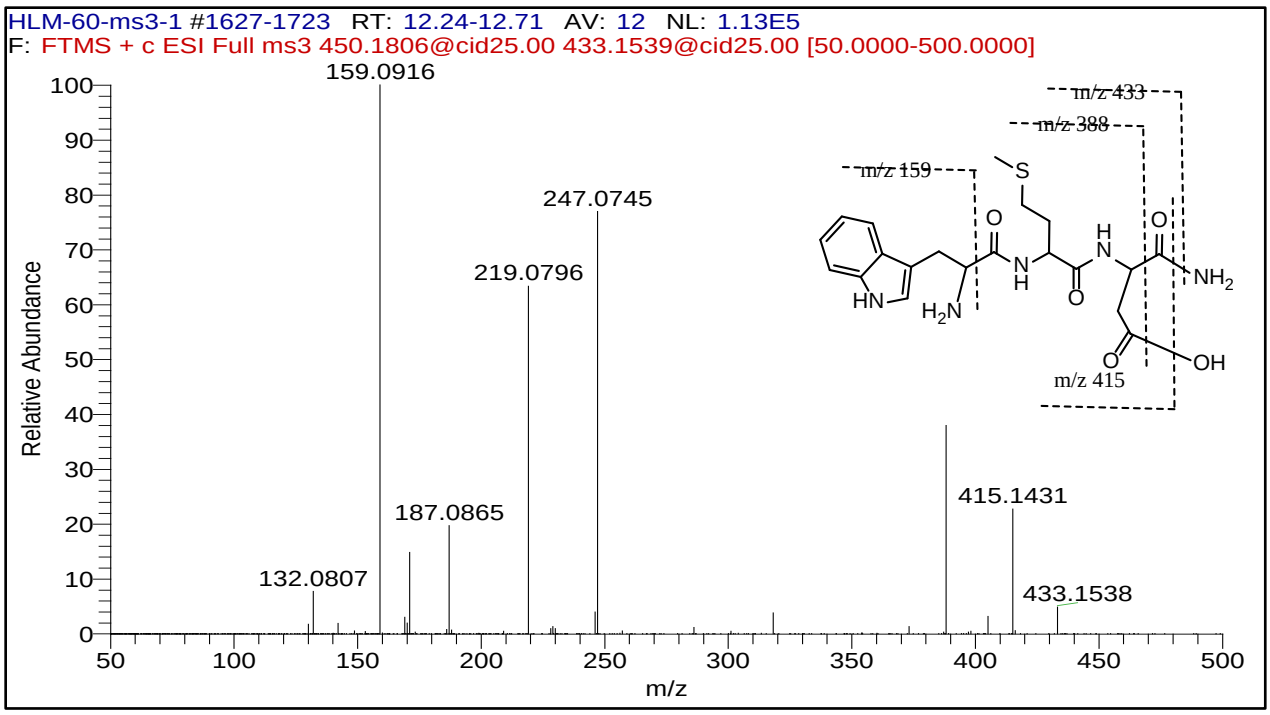

Figure 30. The product ion spectrum of *m/z* 433 from metabolite M8 and proposed fragments.

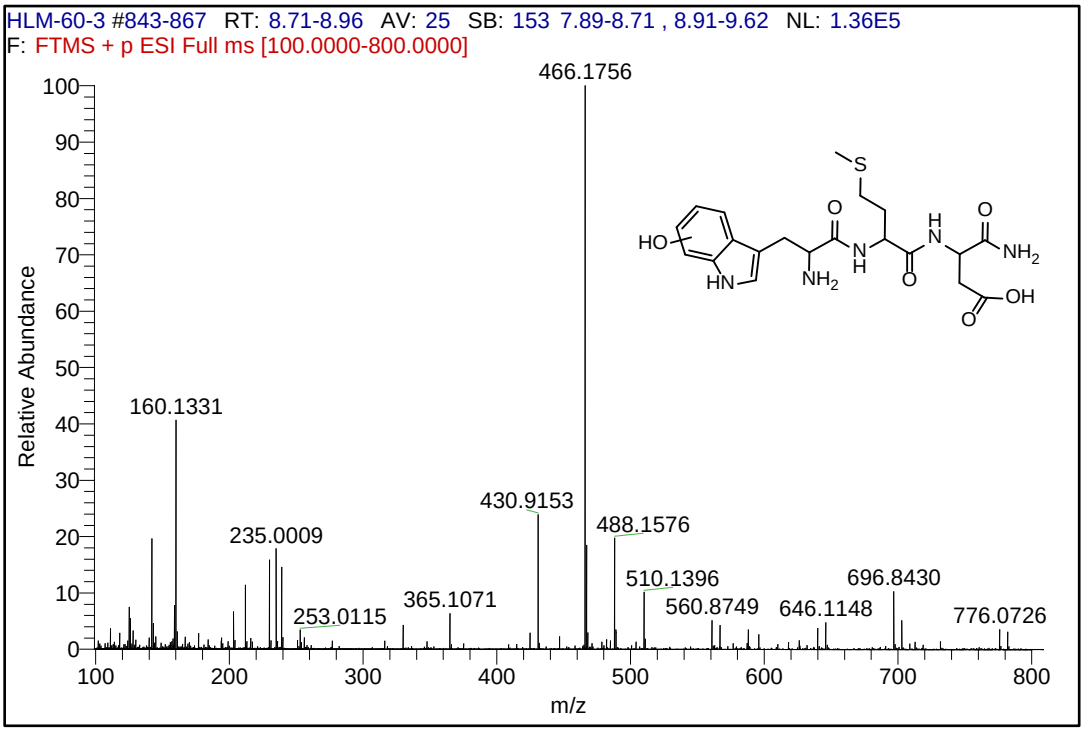

Figure 31. Metabolite M3 (RT 8.82 min) protonated molecular ion at *m/z* 466.

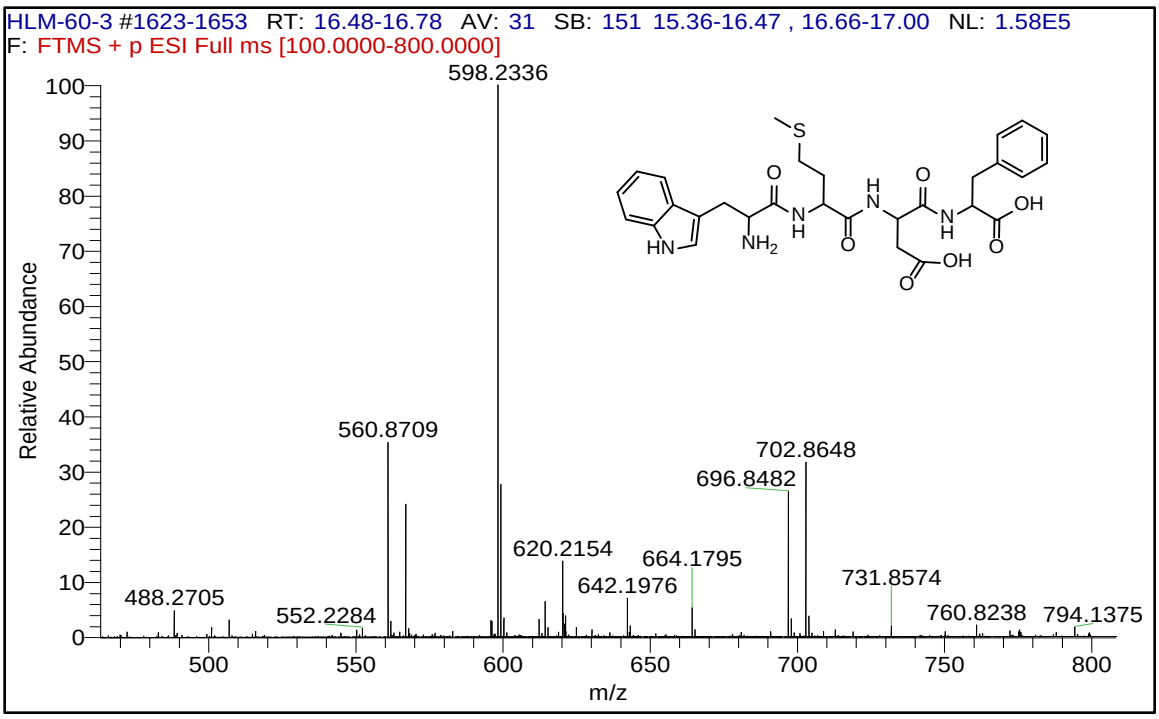

Figure 32. Metabolite M9 (RT 16.56–16.58 min) protonated molecular ion at *m/z* 598.

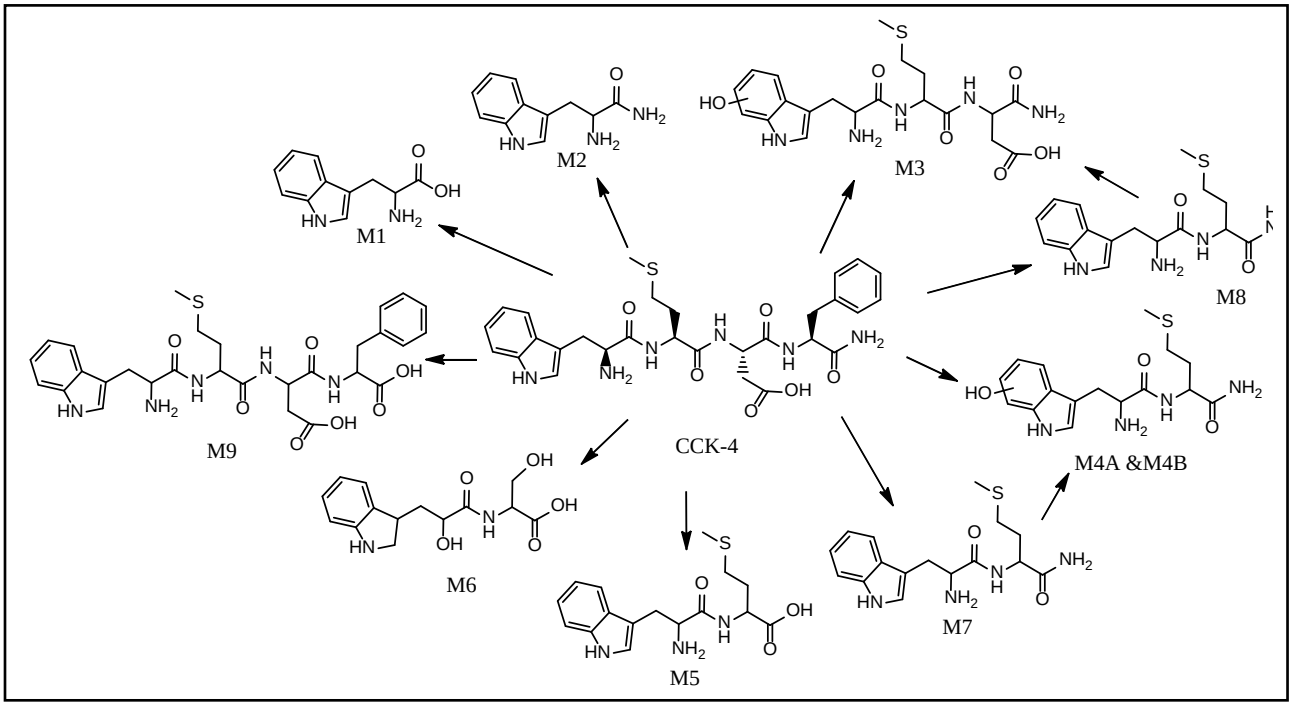

Figure 33. The biotransformation pathway of CCK-4 in HLMs, MyLMs, RLMs, and MsLMs.

Blank

LITERATURE CITED

1. Linden, A. Role of Cholecystokinin in Feeding and Lactation. *Acta Physiol. Scand. Suppl.* **1989,** *585*, i–vii, 1–49.

2. Bradwejn, J.; Vasar, E. *Cholecystokinin and Anxiety: From Neuron to Behavior*; Springer Science & Business Media: Berlin, 2013.

3. Eser, D.; di Michele, F.; Zwanzger, P.; Pasini, A.; Baghai, T.C.; Schüle, C.; Rupprecht, R.; Romeo, E. Panic Induction with Cholecystokinin-Tetrapeptide (CCK-4) Increases Plasma Concentrations of the Neuroactive Steroid 3α, 5α Tetrahydrodeoxycorticosterone (3α, 5α-THDOC) in Healthy Volunteers. *Neuropsychopharmacology* **2005,** *30,* 192–195.

4. Benkelfat, C.; Bradwejn, J.; Meyer, E.; Ellenbogen, M.; Milot, S.; Gjedde, A.; Evans, A. Functional Neuroanatomy of CCK4-Induced Anxiety in Normal Healthy Volunteers. *Am. J. Psychiatry* **1995,** *152,* 1180–1184.

5. Bradwejn, J.; Koszycki, D.; Shriqui, C. Enhanced Sensitivity to Cholecystokinin Tetrapeptide in Panic Disorder. Clinical and Behavioral Findings. *Arch. Gen. Psychiatry* **1991,** *48,* 603–610.

6. Eser, D.; Leicht, G.; Lutz, J.; Wenninger, S.; Kirsch, V.; Schüle, C.; Karch, S.; Baghai, T.; Pogarell, O.; Born, C.; Rupprecht, R.; Mulert, C. Functional Neuroanatomy of CCK-4-Induced Panic Attacks in Healthy Volunteers. *Hum. Brain Mapp.* **2009,** *30,* 511–522.

7. Eser, D.; Schüle, C.; Baghai, T.; Floesser, A.; Krebs-Brown, A.; Enunwa, M.; de la Motte, S.; Engel, R.; Kucher, K.; Rupprecht, R. Evaluation of the CCK-4 Model as a Challenge Paradigm in a Population of Healthy Volunteers within a Proof-of-Concept Study. *Psychopharmacology (Berl.)* **2007,** *192,* 479–487.

8. Schunck, T.; Erb, G.; Mathis, A.; Gilles, C.; Namer, I.J.; Hode, Y.; Demaziere, A.; Luthringer, R.; Macher, J.P. Functional Magnetic Resonance Imaging Characterization of CCK-4-Induced Panic Attack and Subsequent Anticipatory Anxiety. *Neuroimage* **2006,** *31,* 1197–1208.

9. Sugasawa, N.; Kawase, T.; Oshikata, M.; Iimuro, R.; Motoyama, A.; Takayama, M. Formation of c- and z-Ions due to Preferential Cleavage at the NC Bond of Xxx-Asp/Asn Residues in Negative-Ion CID of Peptides. *Int. J. Mass Spectrom.* **2015,** *383–384,* 38–43.

Blank

ACRONYMS AND ABBREVIATIONS

CCK	cholecystokinin
CCK-4	cholecystokinin tetrapeptide
HLM	human liver microsome
LC	liquid chromatography
M	metabolite
MS	mass spectrometry
MsLM	mouse liver microsome
MS/MS	tandem mass spectrometry
MyLM	monkey liver microsome
m/z	mass-to-charge ratio
NADPH	β-nicotinamide adenine dinucleotide 2'-phosphate reduced tetrasodium salt hydrate
RLM	rat liver microsome
RT	retention time
TFA	trifluoroacetic acid
UPLC–HRMS	ultra-performance liquid chromatography–high-resolution mass spectrometry

DISTRIBUTION LIST

The following individuals and organizations were provided with one Adobe portable document format (pdf) electronic version of this report:

U.S. Army Edgewood Chemical
Biological Center(ECBC)
Chemical Sciences
RDCB-DRC-C
ATTN: Kong, L.
Berg, F.

Defense Threat Reduction Agency
J9-CBS
ATTN: Peacock-Clark, S.
Vann, B.

Department of Homeland Security
RDCB-PI-CSAC
ATTN: Mearns, H.

Office of the Chief Counsel
AMSRD-CC
ATTN: Upchurch, V.

G-3 History Office
U.S. Army RDECOM
ATTN: Smart, J.

ECBC Rock Island
RDCB-DES
ATTN: Lee, K.
RDCB-DEM
ATTN: Grodecki, J.

ECBC Technical Library
RDCB-DRB-BL
ATTN: Foppiano, S.
Stein, J.

Defense Technical Information Center
ATTN: DTIC OA


EDGEWOOD CHEMICAL BIOLOGICAL CENTER
A U.S. Army RDECOM Laboratory